Nondestructive Evaluation and Underwater Repair of Composite Structures

by

WILLIAM L. HAGAN III

Bachelor of Science in Marine Engineering Systems
United States Merchant Marine Academy, 1999

Submitted to the Department of Mechanical Engineering in partial fulfillment of the
requirements for the degrees of

NAVAL ENGINEER
and
MASTER OF SCIENCE IN MECHANICAL ENGINEERING

at the

MASSACHUSETTS INSTITUTE OF TECHNOLOGY

June 2008

Signature of Author . . . .
Department of Mechanical Engineering
May 9, 2008

Certified by . . . .
James H. Williams, Jr.
School of Engineering Professor of Teaching Excellence
Thesis Supervisor

Certified by . . . .
Patrick J. Keenan, Captain, USN
Professor of the Practice, Naval Architecture
Thesis Supervisor

Accepted by . . . .
Lallit Anand
Professor of Mechanical Engineering
Chairman, Committee for Graduate Studies
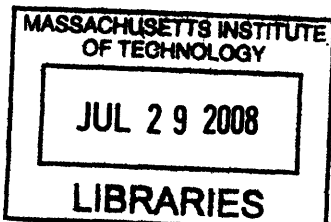
Nondestructive Evaluation and Underwater Repair of Composite Structures

by

WILLIAM L. HAGAN III

Submitted to the Department of Mechanical Engineering
on May 9, 2008 in partial fulfillment of the
requirements for the degrees of Naval Engineer and
Master of Science in Mechanical Engineering

ABSTRACT

Composite materials are gaining popularity in U.S. Naval applications because of their unparalleled strength, stiffness, and manufacturing simplicity. A better understanding of the structural integrity of these materials has the potential to reduce overdesign, decrease manufacturing cost, and simplify repairs.

Though underwater nondestructive evaluation of composites has not been well documented, this thesis illustrates the available technologies for underwater evaluation and repair of laminated composite structures, similar to those currently used in marine applications. Dependent on accuracy and reliability of underwater evaluation, the decision to pursue temporary or permanent repairs may be made based on available information regarding the structural integrity of the effected repairs.

Discussion of the environmental effects on composite laminates and their repairs is included to provide insight into the detrimental effects of contaminates such as saltwater and petroleum products. The effect of the environment has a profound impact on the quality of composite repairs using currently available repair materials.

Underwater repairs, whether permanent or temporary, are suggested for future U.S. Navy components such as the DDG-1000 composite twisted rudder. Furthermore, a suggestion is made to eliminate the use of cofferdams on U.S. Navy shaft covering repairs in order to reduce both cost and the risk of injury associated with a cofferdam.

Thesis Supervisor: James H. Williams, Jr.

Title: School of Engineering Professor of Teaching Excellence

Thesis Supervisor: Patrick J. Keenan, Capt., USN

Title: Professor of the Practice, Naval Architecture

ACKNOWLEDGEMENTS

The past three years at MIT have been an unforgettable experience. The education provided by this institution has prepared me to succeed in whatever opportunities arise. I would like to thank the many people who have guided me along the way:

TABLE OF CONTENTS

LIST OF FIGURES

LIST OF TABLES

1

INTRODUCTION

1.1 Motivation

Composite materials have grown in popularity during the last 50 years, whether in the form of ceramics for mechanical engines, laminate and sandwich composites for ships and aircraft, or simply polymers for repairs. Whether *carbon* or *glass* fibers, fiber reinforced polymeric (FRP) materials provide unparalleled strength, flexibility during construction, and corrosion resistance in harsh environments. Unfortunately, the repair of composite materials to enhance their lifetime durability and structural integrity remains a concern.

Today, composite materials can be found in every facet of daily life. The aerospace industry has developed aircraft that have up to 50% of the fuselage and wings built with composite materials, able to withstand the rigors of flight over thousands of loading cycles [1]. The marine industry has been building ships for more than 30 years using fiber composite materials in small boats to yachts that exceed 150 feet [2, 3]. In each of these cases, there is a need to inspect the composite structure at regular intervals, assess the level of deterioration or damage, and perform corrective repairs.

The book, Salvage Engineering, published in May 1992, is an outstanding reference for the underwater repair industry, which acknowledges shortcomings concerning composites and polymers in underwater and salvage engineering. Salvage Engineering, states that "composite panels are difficult to punch, or shear without

cracking and cannot be hammered or permanently bent" and "there is no reliable method of ensuring proper resin impregnation of immersed fibers" [4].

Since 1992, significant improvements have been made in the field of composites and the time has come to revisit applications in this challenging engineering discipline. This thesis focuses on the need for an updated analysis of the technologies available to engineers and divers qualified to perform underwater damage assessment and repairs.

1.2 Composites in the U.S. Navy

The U.S. Navy's Underwater Ship's Husbandry Manual [5] provides examples of epoxy polymer repairs for surface ship masker/emitter belts, Sonar Rubber Domes (SRD), and propulsion shaft coverings as well as material suggestions for use during emergency situations. Surface ships use a masker/emitter belt to inject air bubbles into the water to disguise their presence from submarines. Damage to the masker/emitter belt may be sustained through improper tug placement when moving in and out of port, corrosion damage, or improper block location during drydocking. Masker/ emitter belt repairs are generally not considered significant enough to warrant drydocking and do benefit from underwater repair techniques using underwater curing epoxy.

Submarine and surface ship Sonar Rubber Domes repairs are qualified as either grooming repairs, requiring only a polymer epoxy, or structural, which employs a combination of patch and epoxy. A grooming repair addresses defects on the outer sonar dome covering such as gouges, pits, blisters, bubbles, flaps and cuts. The Underwater Ship Husbandry Manual requires structural repair procedures for any disbonded rubber flap greater than two square inches or when one or more of the wire plies have been exposed or broken [5].   In either example, HP-2 Elastolock® adhesive is used for bonding.   B.F. Goodrich's NOFOUL® patch is used for structural repairs.   Both

materials are the only approved materials for permanent structural repairs on U.S. Navy sonar domes.

Propulsion shaft coverings provide corrosion protection from the marine environment for the shafts of most U.S. Navy ships. The current coverings consist of four alternately wrapped glass reinforced plastic (GRP) cloth layers impregnated on site with epoxy resin. For an underwater repair, materials must be applied in a habitat free of surrounding water and contaminants. The required underwater habitat is expensive, time consuming, and involves risks due to flood of the habitat during application or curing.

1.2.1 Emergency Repairs

The U.S.S. San Francisco was perhaps the most interesting and challenging salvage problem in 2005. During this project, on-site engineers and divers used more than 25 gallons of epoxy to stabilize a $2 billion dollar submarine and ensure that the ship would not sink at the pier [6]. The U.S.S. San Francisco emergency repair experience paved the way for the repair of the U.S.S. Newport News, a U.S. Navy submarine that sustained damage in 2007 when she was overtaken by a tanker in the Straits of Hormuz. During this collision, the Newport News sustained 17 strikes from the tanker's propeller and lost a significant portion of her forward buoyancy, similar to that of the U.S.S San Francisco. Emergency response plans initially involved the use of epoxy materials until the extent of the damage was known. After a thorough inspection and engineering assessment, steel was chosen for the repair due to the size and extent of the damage [9].

The loss of the U.S.S. Boone's (FFG-28) rudder, November 2006, in the Mediterranean Sea further demonstrates the need to anticipate unforeseen repairs to a ship's component, even if that component was never intended to be removed, damaged, or modified [8]. Subsequently, the entire FFG class of ships required a rudder nut

modification to ensure the rudder nut would not loosen, causing the loss of another rudder. The modification required removing an access plate on the port side of the rudder to facilitate the installation of a cotter pin as a rudder-nut securing device. A new steel access plate was then sized and welded into place [8].

1.3 Thesis Overview

Within a few years the U.S. Navy will have composite surface ship rudders; possibly composite submarine rudders, bow and stern planes; and even entire composite ship superstructures and hulls. Composite materials were chosen for the DDG-1000 superstructure and rudders [10] and have been proposed for the hull design of the MK-V Special Operations Craft Replacement [11]. These examples demonstrate an immediate need for the study of composite and polymeric repairs to ship structures and appendages, and reliable procedures for underwater repairs enabling the U.S. Navy to save thousands of dollars avoiding drydockings and unnecessary maintenance.

The next destroyer class (DDG-1000) and, if retrofitted, the current class (DDG-51) will use a composite twisted rudder (CTR) constructed of a steel frame with a foam core under a 25-layer, *E-glass / Vinyl ester* laminate composite shell [10]. The implementation of a composite material below the waterline raises the question, "Can a composite material be nondestructively evaluated and repaired underwater using current methods?"

This research will reference the use of fiber reinforced plastics (FRP) in the oil and gas industries and the use of underwater nondestructive evaluation (NDE) techniques to ensure proper defect detection, engineering assessment, and repair bonding. Further discussion will address applications for repairing propulsion shaft coverings using materials capable of curing underwater in order to save time and money.

2.1 Introduction

Nondestructive evaluation (NDE) methods have gained popularity as composite materials become more prevalent across industry boundaries. As production techniques advance and composite materials are expected to possess greater strength, resilience, and longevity so should the methods by which their quality is evaluated. Although many more nondestructive evaluation methods exist and will be discussed, the primary methods used by the U.S. Navy's research and development are visual, ultrasonic, and laser shearography [13].

2.2 Nondestructive Evaluation

NDE, in the most general terms, relies on energy transformation in order to assess the condition of the material [14]. Visual or dye-penetrant methods use light energy to reflect indications of defects on material surfaces. Other methods such as ultrasonic imaging, radiographic, or eddy current testing process energy to observe the material structure beneath the surface. In magnetic particle testing a magnet is energized; infrared testing imparts heat energy on to the surface; vibration analysis uses a motor to induce energy into a structure; and acoustic emission testing uses mechanical stress, all to gain a clearer picture of the underlying material properties. In each technique, the energy imparted into the structure produces information that may indicate anomalies

representing defects if present, or no indication if the material is in pristine condition. Regardless of the method used, the goal is to identify areas where damage has been observed or is suspected and thereby obtain a thorough assessment of the structural integrity in order to devise an effective repair strategy.

Most nondestructive evaluation methods can be classified as a pre-repair engineering structural assessment. Prior to nondestructive evaluation, material health and safety could only be determined through sample testing, which could damage the material during the assessment process [15]. These methods for evaluating a material after manufacture or during different service intervals often require components to be taken out of service for extended periods of time depending on the complexity of the part [16]. Conventional pre-repair in-situ, or in place, nondestructive methods evaluate materials in their current state without damage and at minimal cost. However, pre-repair nondestructive assessments have two distinct disadvantages: 1) evaluating a component under unstressed conditions (not dynamic) or 2) artificially stressing the material, as in shearography, to find defects that would otherwise avoid detection such as kissing disbonds.

Active monitoring in-situ nondestructive evaluation methods are relatively new and are increasingly referred to as structural health monitoring (SHM) [17]. SHM evaluation networks can provide real-time data, addressing stress concentrations and material loading, thereby providing clues to material delaminations, hot spots, and barely visible impact damage (BVID), that may otherwise be undetected [16, 52]. NDE data can then be used to change the operating profile, determine appropriate repair size, reduce future material structural overdesign (safety factors), or replace scheduled maintenance with required maintenance [16]. Types of in-situ monitoring include the use of surface-bonded foil resistive strain gauges, acoustic sensors, and fiber optic sensors. These technologies will be briefly discussed later in this work.

The U.S. Navy currently uses *E-glass*, *S-glass*, and *carbon* fiber for both laminate and sandwich composites for ship structures combined with *vinyl ester* resin [13]. Where applicable, NDE methods related to these materials will be highlighted.

2.3 In-Water Inspections

In-water inspections can be subdivided into six categories: inventory, routine, damage, in-depth, interim, and construction [21, 22]. These categories and their underlying procedures have been used primarily for ship structures and bridge pile inspections. Inventory and construction inspections cover the broader marine industry including offshore oil and gas platforms and over-water bridge piles, which are inspected after construction for baseline structural measurements. Interim, routine, and in-depth inspections are preventative maintenance inspections by nature and document the status of material exposed to the marine environment for further engineering repair assessment. The following sections will discuss methods to accomplish these inspections. Inspection of obvious damage, not requiring nondestructive evaluation, will not be addressed.

The American Society of Civil Engineers classifies underwater inspections as such; intermediate and routine visual inspections are termed Level I; while Level II and Level III fall under the in-depth category [22, 23]. For example, U.S. Navy divers are employed for Routine, Level I hull inspections to discover mines prior to entering ports, to assess the hull or appendage, and to verify critical block placement during a drydocking. Hull and appendages assessments begin with visual inspection of the body of a ship and components below the waterline. Further inspection methods are typically warranted only in the case of visible corrosion or defects found during routine inspections.

Level II inspections involve the cleaning of the inspected material surface and noting the location, depth (penetration), and extent of visible defects [22, 23]. Level III inspections entail any number or combination of nondestructive evaluation methods discussed in Section 2.4. Data gathered during Level III inspections are used in a pre-repair engineering assessment of the structure in order to formulate the correct repair methodology, materials, and cost estimation.

2.4 Nondestructive Evaluation Methods

Nondestructive evaluation has developed in many industries to suit the uses of the materials and qualifications of the inspectors. In some cases, science has intervened and produced equipment capable of aiding the inspectors in providing a greater, quantitative understanding of the material structure being tested. Visual, tapping, ultrasonic, dye penetrant, vibration, magnetic particle, eddy current, and infrared thermography are a few of the methods used to inspect materials used in structures today. The following discussion will omit methods with little potential for underwater applications due to either complexity or physical limitations with the underwater environment or operators.

2.4.1 Visual Inspection

Visual Inspection tends to be the first line of any nondestructive evaluation of a structural material [13, 37, 38, 52]. Visually inspecting a specimen can be as simple as using a flashlight at an angle that may highlight surface defects or as complex as aiding the inspector with tools such as magnifiers or dental picks [24]. Airbus states: "from a distance of approximately 6 ft and using a flashlight to illuminate the area, surface damage with an area of 0.002 in.^{2} and a depth of 0.012 in. was reliably detected (95%

probability)" [25]. The U.S Department of Transportation [24] sites the main factors in reliability of visual inspection to be:

- Physical factors (personnel):
  - o Visual acuity, boredom/rest, attitude, vigilance, and experience
- Environmental factors:
  - o Task complexity, fault or flaw size, lighting, and visual noise.
- Managerial organization:
  - o Work duration, inspection time allotted, and social pressures.

While most of the findings in the Department of Transportation's report are of little significance, two points are interesting:

- As the size of the fault increased from "tiny" (3 mm) to "huge" (7 mm), the probability of a search error decreased by more than 50 percent. However, the change in inspection speed was not seen to be as dramatic for the various fault sizes.
- The inclusion of either one or two defects had no effect on inspection effectiveness. On the other hand, it was determined that prior knowledge of defect types and inspector age was statistically significant.

The study concluded with the recommendation for all inspectors to be regularly reeducated on the types of defects expected in each specific material.

An underwater evaluation of remote visual testing (video camera) methods has found crack width or defect size to be the primary factor in success of visual inspection [38]. This evaluation was conducted in a nuclear facility using ceramic specimens. Figure 1 shows results according to the observer's certainty level: positive crack, possible crack, probable - no crack, and definite - no crack (DNC). Lenient counted all positive,

possible, and probable flaw indications. Normal counted both definite cracks and possible cracks. Strict counted only definite cracks. These results highlight the possibility of detecting cracks underwater versus the crack width.
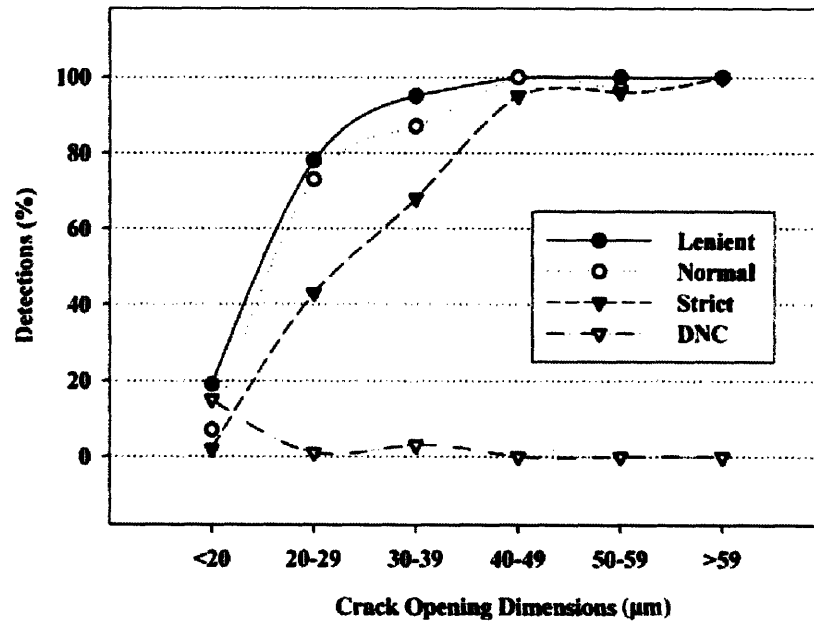
Figure 1: Crack width versus detection underwater [38].

In the marine environment there is the concern of moisture penetration, especially in the underwater environment similar to that which the DDG-1000 *E-glass / Vinyl Ester* rudder and shaft coverings will be exposed. Specifically, in an underwater environment limited visibility, distortion caused by the diver's faceplate, thermal gradients (similar to heat rising above a hot road), and fogging of the faceplate are factors that may hinder an inspector's results [5]. Although visual inspection is subjected to a number of underwater factors and can only determine surface defects, successful visual inspections provide justification for their continued use.

2.4.2 Tap Test

Few inspection methods are easier to understand than the tap test method, with the exception of the visual method as discussed previously. As a hard object, coin or washer, strikes the surface of a laminate or bonded surface, the noise reverberates back to the inspector's ears with either a high or low pitch. As the noise is contrasted to surrounding specimens, a low pitch or hollow sound may be heard in the presence of delaminations or moisture intrusion where- as a high pitch would indicate a relatively solid material with a good bond [25, 26, 37, 52, 101].

Although advances have been made to automate the tap testing method, a simple coin is best used for quick and inexpensive initial investigations in conjunction with the visual method [15]. Limitations of tapping are due to the sensitive nature of the bonded materials, being careful not to damage the laminate while striking, and the slow process for testing large areas even with the most experienced inspector. Effective defect mapping can require tapping at very close intervals. Tapping can generally be effective with thin structures and for locating delaminations just below the surface, thus defects in thicker marine structures may be elusive.

Underwater application of this method is less attractive due to sound attenuation underwater and the inability to distinguish slight changes in sound pitch and direction. Further, tap testing would be rendered virtually impossible when diving with a helmet due to the ambient helmet noise caused by exhaust air discharge.

2.4.3 Magnetic Particle Testing

Magnetic Particle testing is the most widely used underwater nondestructive testing method. This method is capable of revealing cracks and porosity in most metals,

but is particularly suited for ferritic weld inspections. Several references incorrectly state magnetic particle testing's incompatibility in the wet environment [31, 32]. Orientation of a magnet will reveal cracks in a direction perpendicular to the flux field as demonstrated in Figure 2. By using heavy magnetic particles observable in water, the defect will attract the particles when electricity is applied to the magnet.

Magnetic Particle inspections have several disadvantages: First, and most prominent, is the need for a strong magnetic signature for the best results. While it could be effective for *carbon* fiber reinforced plastics, the likelihood of success is not high. Second, magnetic particle inspections over large areas are very time consuming considering the small area observed under the magnet. Removal of surface coatings is recommended for the best results and virtually required with coatings in excess of 200 mm because of magnetic field losses [31].

This method has been effectively used in the underwater environment and found to be reliable in assessing 1.5 mm cracks in steel as early as 1980 [31].
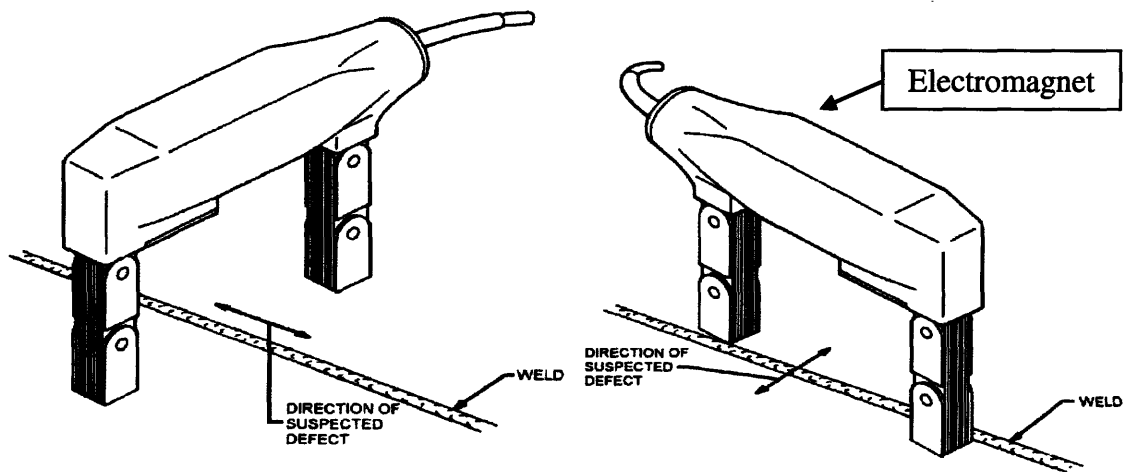
Figure 2: Magnetic Particle Weld Inspection [5].

2.4.4 Dye Penetrant

Dye Penetrant inspections are conducted by applying a surface dye and powder developer to a composite material, and rinsing with water to reveal cracks, blisters, or resin flaking [26]. Because the dye penetrant adheres to the surface defects and penetrations, this method can be used on composite materials where magnetic particle testing cannot. The typical procedure calls for drying the composite surface, applying a powder, drying or baking the surface, then rinsing the excess penetrant from the surface leaving only the defect indications, especially observable under UV light.

Though the open literature does not specifically address the underwater environment, the use of a dye penetrant underwater, in the current form, is unlikely due to procedural issues.

2.4.5 Acoustic Emission

Acoustic emission (AE) monitoring observes the audible and ultrasonic waves transmitted through a structure as it is mechanically stressed by compression, tension, or shearing [14, 15, 28, 34, 37, 52]. As the waves travel through the structure, acoustic wave frequencies encounter changes in thickness, moisture content, or other defects. The frequency changes are monitored using sensors on the material's skin covering both the audible and ultrasonic ranges. Although AE will detect faults throughout the thickness of the material and provide defect localization, the major disadvantage lies in the network of sensors required for location accuracy and the erroneous noise that affects quality measurements.

Acoustic Emission monitoring is unlikely to be widely used by the U.S. Navy because of underwater environmental factors and the sensitivity of the equipment used to observe the structure.

2.4.6 Infrared Thermography

The Infrared thermography technique is one of the fastest growing and most widely accepted methods used in aerospace fields today where thin aerospace composites are used extensively [26, 29, 37, 101]. When a composite material is subjected to radiant heat, heat energy will diffuse through the skin uniformly if no delaminations, foreign matter, or disbonds exist. This temperature diffusion can be easily observed with the use of an IR camera capable of greater than 60 Hz frame rates to capture images of heat diffusing through the material skin. If a defect or impurity does exist, heat transfer will be inhibited causing the IR thermography to produce a high temperature indication or hot spot on the heated side and a cold spot on the back surface [27, 52].
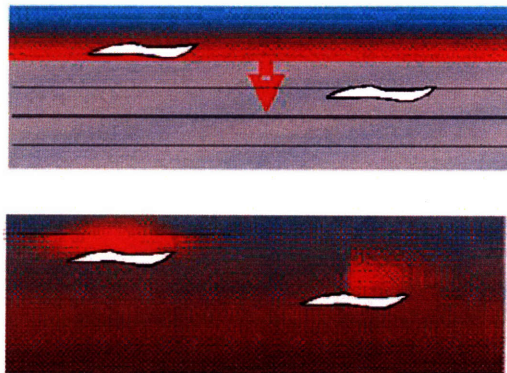
Figure 3: IR Thermography Defect Location [29].

Sensitivity of IR thermography is best described by the defect diameter/depth ratio illustrating that the best observations will occur in thin materials. Generally, the

minimum detectible abnormality possesses a ratio greater than 2; i.e., a 2mm defect at 1mm depth is likely to be detected [29, 30].

IR thermography has several benefits with composite materials, more so than with bare metals which have a relatively low emissivity [25, 29]. Conversely, *carbon* fiber reinforced plastics (CFRP) have a high emissivity causing diffusion to occur more rapidly than *glass* fibers [30]. Diffusion of heat energy in CFRP travels parallel to the material skin preventing the localization of disbonds or delaminations oriented parallel to the surface.

While infrared thermography has many uses in the aerospace industry and enables the inspection of large areas in a short time, the application of this method underwater does not appear to be possible due to water interference with both the heat diffusion and the IR camera observation. The author believes heating elements could be placed at close range to effectively heat a composite structure; however, an IR camera will have difficulty observing a large area due to rapid environmental heat absorption. Increased distance from the subject may hinder an accurate observation and elevate measureable abnormalities to a size more easily detected by prior visual inspection.

2.4.7 X-Radiography

X-Radiography, or X-ray, inspection methods use radiation from an emitter, which passes through the subject, producing an image on film on the opposite side of the subject [22, 26, 30, 37]. X-Ray inspection techniques are known to produce quality images as radiation is stopped by higher density material, yet passes through a surrounding material similar to the contrast between bone and skin on a doctor's x-ray [52]. Depending on the material composition, the x-ray source and exposure times will be adjusted for ideal resolution and penetration.

X-ray inspection methods are most effective detecting transverse cracks, honeycomb damage in sandwich panels, and moisture ingress [25, 30, 37, 52]. Limitations occur with defects oriented perpendicular to the radiation source such as delaminations that do not produce large voids in the material. *Carbon* fiber reinforced composites are known to produce poor x-ray images because of the similar absorption properties of *carbon* fibers and the resins used to bond them, resulting in images that provide little insight. However, *boron* or *glass* fibers are particularly suited for X-ray evaluation.

X-ray inspections have been widely used in the underwater environment for several years [22]. The most significant challenge facing the use of radiography is operator safety relating to exposure to radioactive particles. In order to overcome this safety aspect, automation has been used to open the source emitter during inspection and close it prior to the diver's re-entry into the radiation field. A second challenge exists in arranging the equipment and film relative to the subject. In most cases, extensive preparation time to set up equipment around the specimen is required; and, this could be exacerbated in the underwater environment. Attachment of the film to the opposite side of the subject has been accomplished through the use of magnets on metallic structures or by strapping a film cartridge to the specimen for non-metallic subjects.

2.4.8 Eddy-Current

Eddy current testing is based on the principle of sending an alternating current through a coil in close proximity to a material surface [26, 30, 31, 32]. This method is a proven success on metals with an 87-100% agreement with magnetic particle inspection; however, due to the eddy current probe testing only the area beneath it, the magnetic particle method is capable of inspecting a much larger area [31]. Conversely, magnetic

particle requires a clean surface for visual observation where as eddy currents can penetrate a thin layer of paint over most specimens.

In most conductive materials, a disruption in the magnetic field will indicate a defect in the material; a defect that can be displayed on a cathode ray tube (CRT). Eddy currents do not penetrate deeply into the laminate, but can be used to locate delaminations in the surface layers and are best at locating barely visible cracks, fiber breakage, and impact damage [37]. This method requires electrically conductive materials, therefore limiting it to use on *carbon* fiber based laminates or metals. Due to the depth limitation, eddy current inspections are best coupled with another method such as ultrasonic inspections for deeper penetration observation.

Although available research on eddy currents [31] is unclear whether the tests took place in a controlled laboratory environment or underwater, the results exceeded magnetic particle inspections, detecting imperfections with an average size of 0.4 mm through paint. Speculation as to the adaptability of testing equipment in wet environments for underwater application has been mentioned with the use of Hall Effect probes [22]. Hall Effect probes combine aspects of magnetic particle inspections and the observation of magnetic flux lines similar to eddy current inspections.

Eddy current inspection methods have been tested underwater, but are not currently used by the U.S. Navy diving community.

2.4.9 Ultrasound

Ultrasonic methods are the most prevalent inspection techniques for nondestructive evaluation of composite materials because of the in simplicity and acceptable penetration depth [15, 25, 33, 34, 37, 52]. Ultrasonic inspection typically uses waves between 0.2 and 1.5 MHz for *glass* fiber composites and higher frequencies,

5MHz, for **carbon** fiber composites [13]. By observing the pulse-echo or transmitted through-thickness wave, the depth and size of a defect may be determined [26, 30].

The pulse-echo ultrasonic method is the most common for portable applications; through transmission methods require two-sided access [25]. In addition to defect depth or material thickness, the pulse-echo method is particularly suited to observe both matrix cracking and subsurface porosity [37]. Ultrasonic methods occur in three different image types: A, B, and C-scans [25, 52]. Simple thickness measurements or defect location are known as "A-scan." A combination of A-scans correlated to location along the surface to determine the areal extent of defects or damage is termed "B-scan." The most complex image is called "C-scan." C-scans produce a picture of the internal structure at differing depths by varying the data acquisition time. Figure 4 illustrates the pulse-echo method and provides a display of the expected A-scan CRT image at the defect location.

Through transmission methods use a separate transmitter and receiver and have the advantage of observing the thickness of a material in its entirety on one pass versus a pulse-echo method. Through transmission methods are particularly suited for observing fiber breakage and delaminations [37]. Required access to both sides of the specimen prohibits the use of this method in many circumstances.
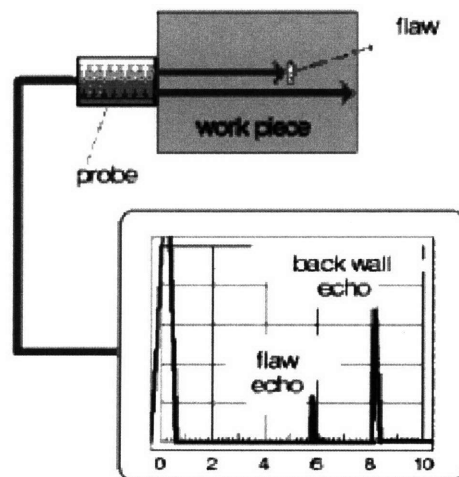
Figure 4: Pulse-echo inspection method [41].

Ultrasonics, while thoroughly tested and widely accepted, have several shortfalls. Figure 5 provides an example of a particular specimen containing multiple defects and the shadowing of one defect by another in the wave transmission path [52]. Honeycomb structures present similar problems due to the different impedances between air and structural materials [25]. Additionally, kissing-disbonds (delaminations without air gaps) are difficult to detect with ultrasonics, as is moisture ingression due to the absorption of energy, preventing wave reflection or transmission.
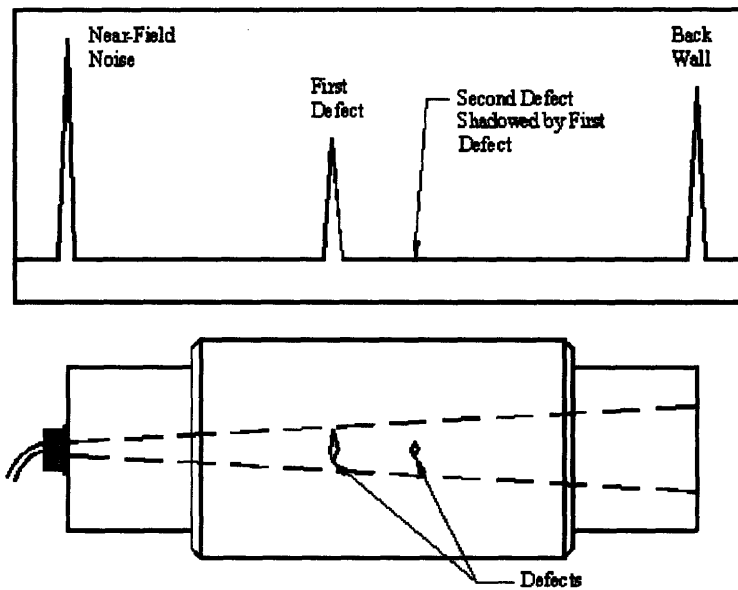
Figure 5: Pulse-Echo Defect Masking [42].

Ultrasonic A-scan inspection methods have been used in the underwater environment for many years for thickness gauging of ship hulls and pipe walls [5, 22]. Ultrasonic probes have also been used to measure tolerances on bolt elongation during the tightening of propeller blade bolts to the propeller hub [5]. The open literature does not address the development of an underwater C-scan device, equipment that would be very beneficial for inspecting the DDG-1000 rudder.

2.5 Underwater NDE Accuracy

Since their conception, underwater nondestructive methods have been studied for accuracy, consistency, and reliability [35]. In a 1984 experiment, the most recent published study found, divers evaluated a number of steel samples at a depth of 12 meters in relatively good diving conditions; i.e., good visibility and minimal current. Using three primary methods of underwater nondestructive testing available at the time: magnetic particle inspection (MPI), ultrasonic testing (UT), and eddy current testing, this experiment addressed the accuracy of detecting cracks in steel samples. MPI trials were used to determine the accuracy of the method using seven different manufacturers' equipment to detect fine, short cracks on the specimen's surface. Ultrasonic testing included the traditional A-Scan method for flaw location, size, and accuracy and a digital method, which measured only thickness. Eddy current testing was performed on two different specimen groups for crack location and length.

The first round of testing conducted in this experiment used specimens containing milled groves or fine cracks in the surface, approximately 5mm in length. Milled grooves were chosen to simulate the loss of material through erosion and corrosion caused by galvanic reaction with saltwater and the removal of marine growth. Accuracy of the MPI testing was shown to fall within the range of 65% - 95% for detection and similar results for size. Ultrasonic scan did not perform as well as the MPI and produced a detection range of 15% - 50%. However, the ultrasonic thickness measurements proved to be more accurate; 70% - 85% accurate within 1 mm (A-scan) and 66% - 92% (digital A-scan). Sample MPI results are shown in Figure 6 with a comparison to actual destructive test results.

A second round of testing limited evaluation to a single specimen series (termed type N) and measured the results against data taken in an above water inspection. Both

above water MPI and ultrasonic tests produced results with a 92% - 100% detection rate for defects and a 14% - 78% accuracy for determining defect size compared to destructive inspection. The underwater MPI results, combined with the first round of MPI testing, show an 89% detection success rate and 15% - 50% accuracy for determining defect size. Ultrasonics produced a minimum of 75% and a maximum of 83% for detection with a maximum overlap success rate between 12% and 44%. The Eddy Current method had similar success during defect detection; 71% - 80%. However, the accuracy of determining defect size compared to destructive inspection was much lower; 10% to 39%. Eddy current inspection data was either not completed above water or not presented in the literature.
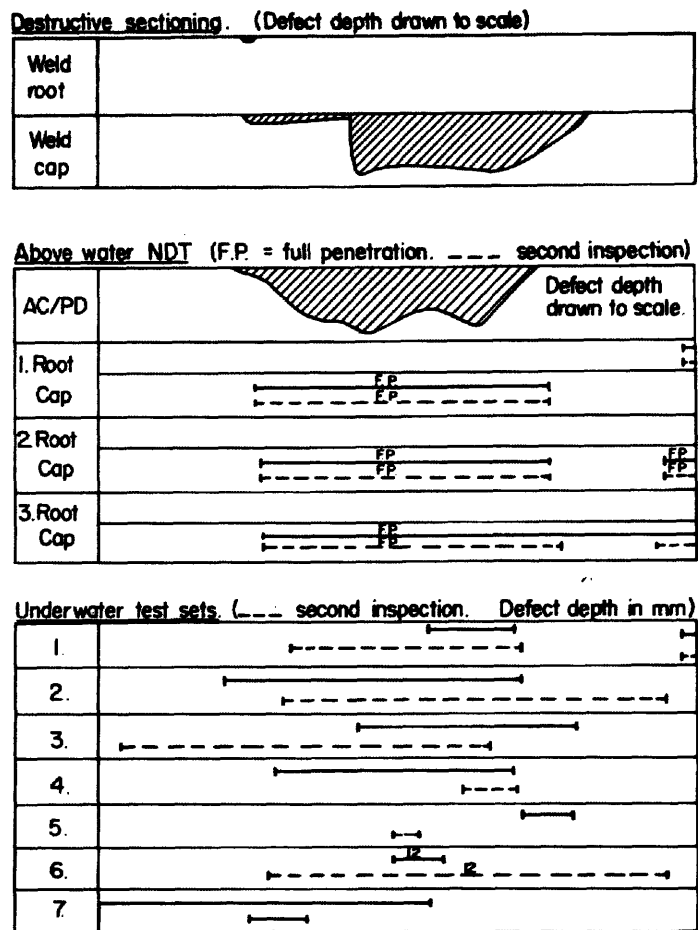
Figure 6: Destructive testing compared to underwater NDE techniques [35].

Figure 6 provides underwater detection results. Defect size and location for one specimen, as determined by destructive testing, is shown at the top and compared to above-water and underwater nondestructive inspections with multiple manufacturer's equipment. The accuracy was then calculated by comparing the underwater results with destructive observations for each specimen. Averaged data from the experimental results discussed in this experiment have been provided in Figure 7. The above water inspections show higher rates of detection and accuracy.
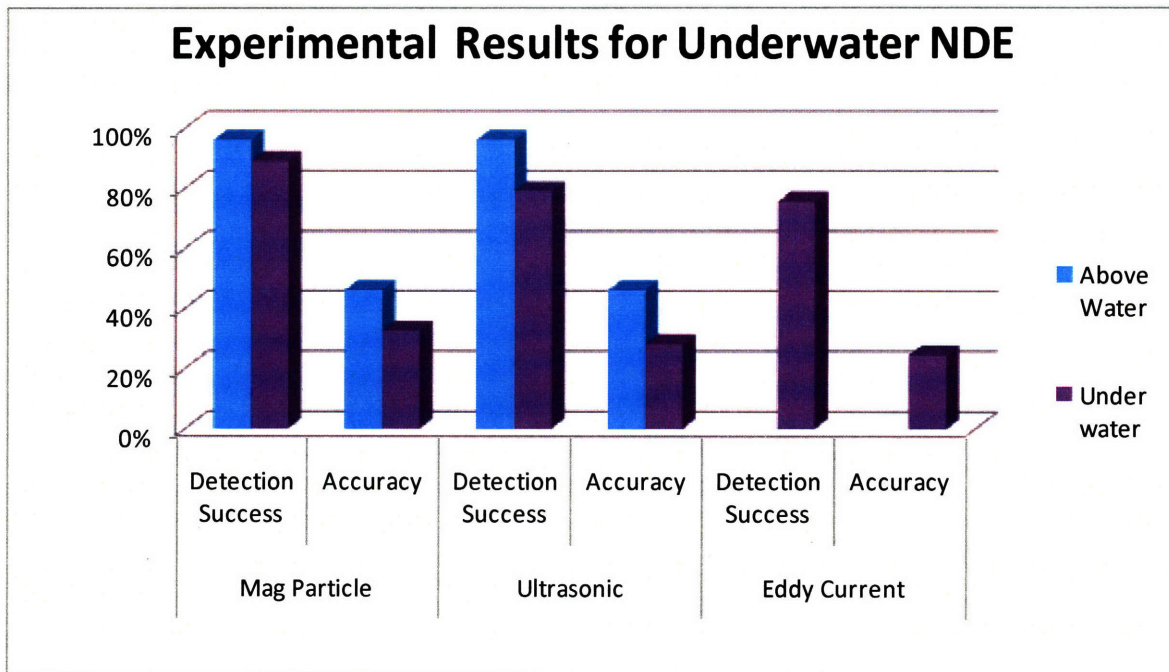
Figure 7: Comparison of underwater methods to above water results [35].

2.6 NDE Summary

Technology for nondestructive evaluation has matured over time, but no single technique is capable of an all-encompassing assessment of the composite structure.

Table 1 summarizes the NDE methods discussed in the previous sections and relevance to underwater applications.

Table 2 provides primary observations for the method specified and whether underwater assessments have been accomplished or have applicability to composites underwater.

The previous discussion has referenced many sources within the aerospace, oil and gas, nuclear, and the nondestructive laboratory testing fields, most of which focused on ferritic materials. Very little information has been published pertaining to underwater NDE and even less concerning composite material assessments in the underwater realm. The major concern with nondestructive evaluation/testing is accuracy regardless of above-water versus underwater environments or metal versus composites [23].

In a dry environment, the aerospace industry expects nondestructive methods including ultrasonic, eddy current, and X-ray to detect all cracks and deformities greater than 4.5mm in length [17]. The primary underwater nondestructive evaluation methods currently used by the U.S. Navy are visual, magnetic particle, and ultrasonic [5]. An open literature search discovered a single published underwater accuracy test concerning NDE methods; it is discussed in Section 2.5.

Table 1: Underwater inspection methods.

Underwater Inspection	Visual	Tap Test	X-Ray	Magnetic Particle	Dye Penetration	Acoustic Emission	IR Thermography	Eddy Current	Ultrasonic (Pulse-Echo)	References
Steel / Metals	Y	-	Y	Y	-	-	-	Y	Y	5, 22, 25, 26, 30, 37, 38
Composites	Y	-	*	Y (CFRP)	-	-	-	Y	Y	

Y: Method has been applied underwater
(*): Method has potential for composite evaluation
(-): Unlikely due to undewater environment

Table 2: Underwater NDE methods, observations, and assessments.

	Too much resin	Folds	Porosity	Foreign Body Inclusion	Delamination / Impact Damage	Cracks	Lack of adhesive (void)	Inadequate cohesion (kissing disbond)	Moisture	References
Visual	*	Y	Y	*	Y	Y	Y	N	-	25, 37
Tap Test	-	-	-	-	Y	N	Y	N	-	25, 37
X-Ray	Y	Y	Y	Y	Y	*	Y	N	Y	25, 26, 36, 37
Magnetic Particle	-	Y	Y	Y	-	Y	-	-	-	36, 37
Dye Penetration	N	N	*	N	Y	Y	*	N	-	26
Acoustic Emission	-	-	N	N	*	*	N	*	-	25, 26, 37
IR Thermography	N	N	N	Y	Y	N	Y	N	Y	25, 26, 36, 37
Eddy Current	-	-	-	-	Y	Y	-	-	-	25, 36, 37
Ultrasonic (Pulse-Echo)	N	*	Y	Y	Y	Y	Y	-	Y	25, 26, 36, 37, 39

Y: Use documented on composites
N: Use has not been documented on composites
(*): Possibility exists for use on composites
(-) : No known composite application

CHAPTER

3

COMPOSITE DAMAGE ASSESSMENT & ENVIRONMENTAL EFFECTS

3.1 Introduction

Damage assessment is perhaps the most critical stage in a repair regardless of the material involved. Ultimately, nondestructive evaluation leads to an educated evaluation of the structural safety, remaining service life, and possible consequences if the material were to continue service. An accurate damage assessment will determine if a repair is justified and, if so, the extent of damage to the surrounding area, repair method, and the associated cost.

In industries where steel is the prevalent material, transition to composites can be overwhelming and repairs may seem impossible. Steel based industries are familiar with low-technology repairs performed by personnel with relatively little training. By contrast, composite materials traditionally require laboratory environments and highly skilled technicians. These differences make understanding damage assessment and repair techniques essential for prolonging the life of composites.

3.2 Damage Assessment

Damage assessment and composite repairs revolve around a number of factors including damage location, load requirements for the structure (tension, compression, or torsion), operational and repair environments, and available resources [30].

Traditionally, larger ships require drydocking; events scheduled far in advance for regular ship maintenance and may not be available in an emergency. Smaller vessels requiring repairs may be subjected to trade-offs between repair cost, dictated by the extent of damage and repair method, and vessel cost. Additionally, compatibility between repair materials, existing structure, and environmental factors (moisture and contaminants) must be considered. For example, repairs conducted in field conditions rather than a controlled laboratory environment require resins and adhesives capable of curing at lower temperatures and bonding to contaminated surfaces.

Composite damage can be classified in different categories depending on criticality of the application, size of the area affected, and repair type. Initially damage is classified as damage with or without skin penetration and environmental or fatigue degradation damage [37]. The aerospace industry's structural repair manual (SRM) further classifies damage in conjunction with specific repair levels: allowable damage, damage for which temporary and incomplete repairs are acceptable; repairable damage; and non-repairable damage [25, 30]. The Handbook of Adhesive Bonded Structural Repair simply categorizes repairs as temporary, semi-permanent, and permanent [40]. Although confusing at times, terminology clearly does not affect the level of repair as much as the area in question or the damage types.

As discussed in Chapter 2, there are a number of damage types, most of which can be repaired depending on the criticality of the structure and its' location in the overall system. For example, the allowable hull repair area beneath the waterline should be smaller than that allowed on a composite superstructure above the waterline. Similarly, in the aerospace industry, a flap or actuator hinge under constant stress may be more critical and complicated than a wing panel section [25]. The U.S. Air Force specifically restricts bonded repairs on critical components to instances where the remaining structure is below the ultimate strength at limit load [44]. As a rule-of-thumb, a part is

recommended for removal if the damaged area exceeds 50% of the part area [25]. Boeing limits low temperature (200 – 230°F), wet lay-up honeycomb panel repairs to less than 50% of the smallest dimension across the damaged part, but has no size limit for 350°F cure temperature repairs. Specimens damaged beyond these limits may exceed financial incentives to repair the components and should be scrapped.

Other than size of the affected area, damage methods and skin penetration are principal factors concerning the repair type. Different damage methods include, but are not limited to: abrasion, chemical attack, fracture/cracking, delaminations, disbonds, erosion/corrosion, and impact damage [25, 40].

3.2.1 Minor Damage without Penetration

Minor damage without penetration is a feasible candidate for underwater repairs if moisture intrusion is not suspected through matrix crazing or surface cracks. The best solution for this is underwater curing epoxy or pre-preg composite layers capable of restoring minimal strength loss.

Cosmetic damage may appear to be insignificant, but actual subsurface damage should be assumed to be more extensive than appears on the surface, as is the case with *carbon fiber reinforced* composites [37]. Visible damage such as small dents may have negligible effects on structural properties of the composite and may be repaired with an appropriate compound to restore strength and aerodynamic or hydrodynamic properties. Incidentally, topside structures with a significant number of contour changing defects may increase the radar observable signature of naval vessels. This could be a detriment to the current DDG-1000's *carbon fiber reinforced* superstructure that has been designed with continuous, smooth surfaces for near-stealth capabilities.

3.2.2 Damage with Skin Penetration

While damage without skin penetration is detrimental to the strength properties, moisture intrusion through a penetration may have even greater consequences. As bonding adhesives are exposed to moisture, the bond strength weakens as plasticization occurs [37, 46]. Evidence suggests that exposure to a 5% salt spray solution for 3 months may be more damaging to adhesive bonds than exposure to semi-tropical, high humidity conditions for three years [30]. Thus, moisture intrusion damage must have immediate attention to prevent further deterioration that may lead to premature failure. If the damage is considered recent, the moisture ingestion may be relatively small depending on the location of the defect; above or below the waterline. Chapter 2 of this thesis addresses methods for successfully determining moisture intrusion in composite materials.

Figure 8 provides experimental data for the mass gain as a function of time for *E-glass / vinyl ester*, 3-layer woven roving sandwiched between 4-layer chopped strand mat (4C3W), 4-layer woven roving (4W), and neat *vinyl ester* specimens submerged in a 2.5% saltwater solution [50]. In general, saturation was reached at 28 - 30 weeks with neat resin showing higher moisture absorption than the composite specimens. The percentage weight gain differences in the composite specimens are attributed to lower fiber volume content and greater concentrations of resin rich deposits due to chop strand mat inclusion.
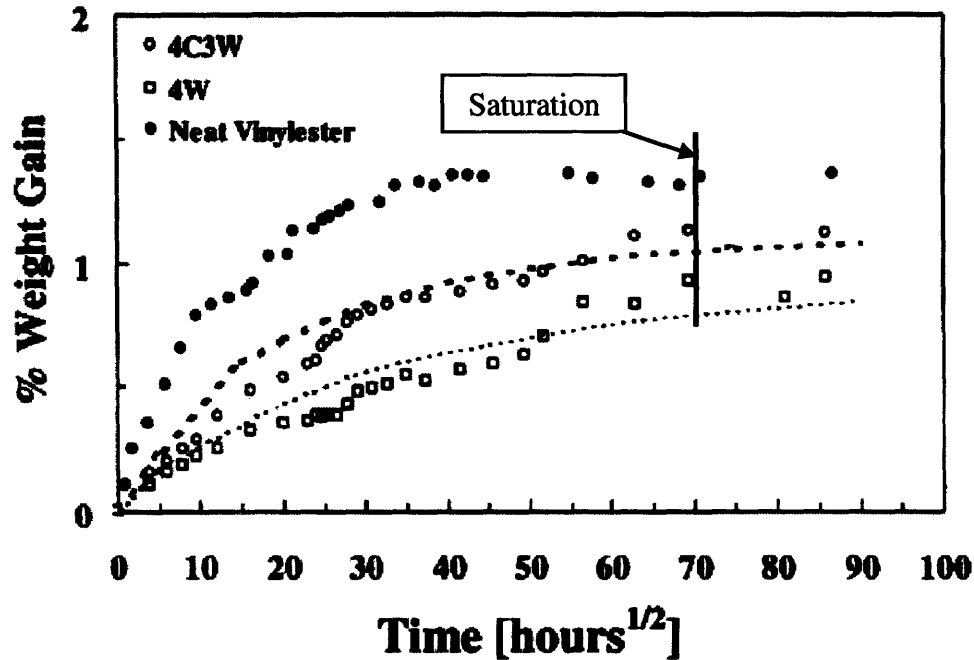
Figure 8: Mass gain over time for composites immersed in saltwater solution [50].

Although chopped strand mat is recommended to provide smooth surfaces, their increased moisture absorption characteristics affect strength retention under tensile loading and suffer adverse fatigue life affects due to plasticization.

Water absorption occurs in three stages; first, diffusion according to Fick's law, where water permeates into void spaces; second, bonding interactions between water and the polymeric matrix; and third, water absorption by composite fibers [46, 55]. Figure 9 illustrates the relationship between *E-glass / vinyl ester* composite materials and their resistance to interfacial shear (τ_r), and flexural modulus (E_r) after submergence in distilled water relative to a pristine sample. Similar to Figure 8, Figure 9 shows weight gain due to water absorption, but provides additional insight to the plasticization of the material by observing the degradation of modulus and shear resistance concurrently.
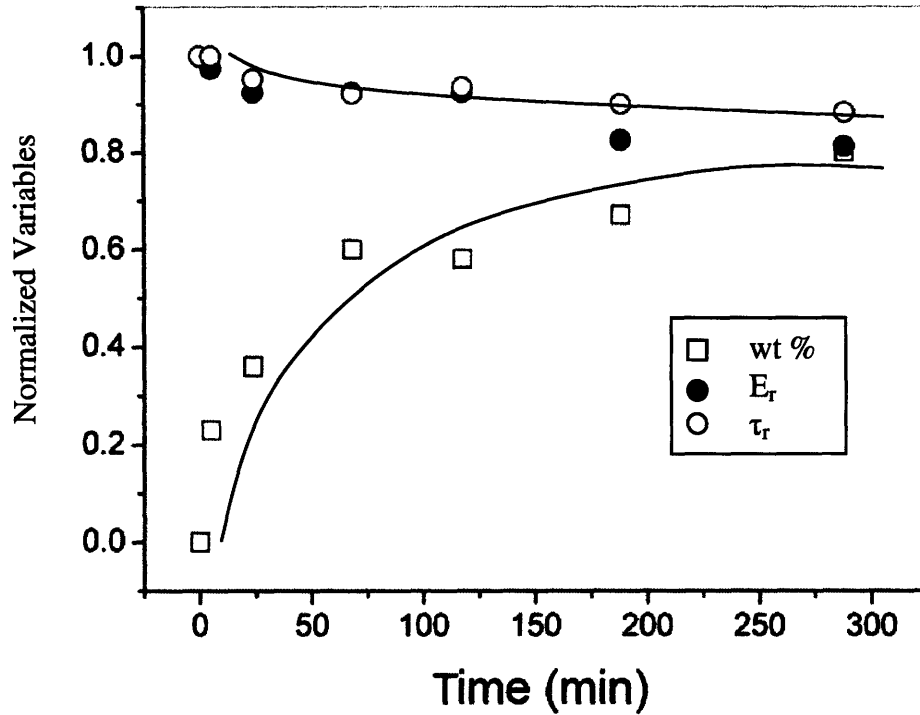
Figure 9: Water absorption for mat composite, glass fiber / vinyl ester [46].

3.3 Moisture Intrusion Effects on Composite Materials

According to the article, "Environmental Effects on Composites," moisture effects reduce *polyester* laminate strength by 10-15%, while *epoxy* resins are less susceptible [37]. Experimental results show similar findings for *vinyl ester* composite laminates [46, 50, 53, 54].

Figure 10 and Figure 11 provide data for 4W and 4C3W for reduction of tensile strength and tensile modulus after immersion in 2.5% salt solution and regained strength after drying (desiccation) [50]. The 4W data from initial measurements to the 11 month saturation show a 25.5% tensile strength reduction and a 14.9% tensile modulus reduction; 4C3W, although lower overall values, showed strength and modulus reductions of 14% and 10.1%, respectively.
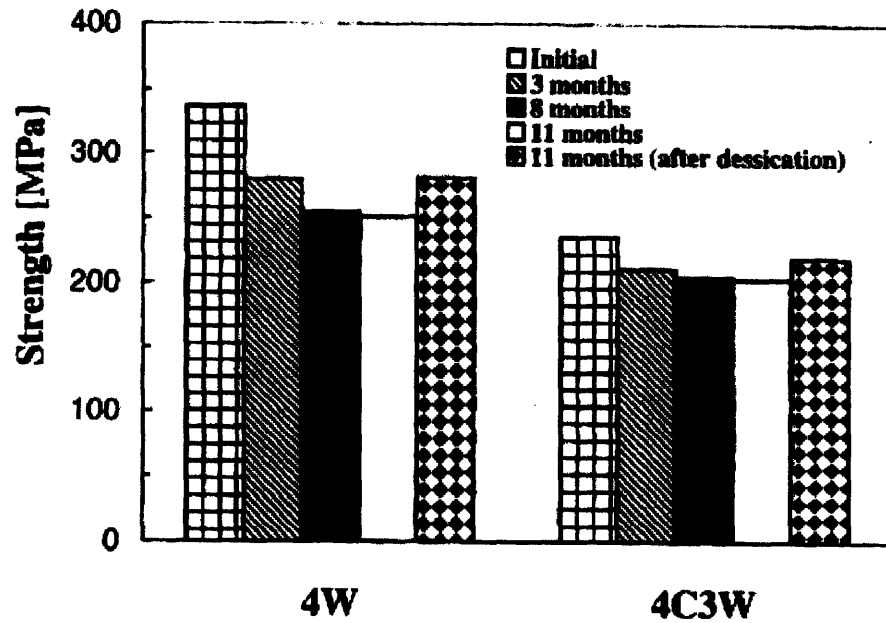
Figure 10: Retention of strength after immersion in salt solution [50].
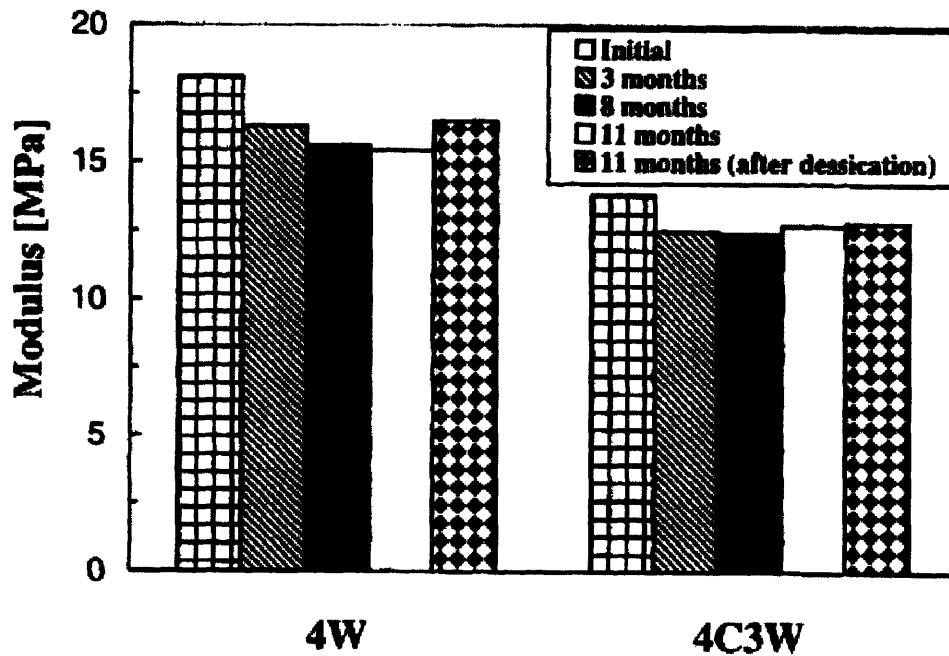
Figure 11: Retention of flexural modulus after immersion in salt solution [50].

Further comparison of saturation time and the asymptotic degradation point reveals that strength and modulus reach minimum levels at 28 – 30 weeks in both specimens. 4C3W samples with higher resin content retained more tensile strength and tensile modulus than

the 4W woven mat. Subsequently drying the samples resulted in partial restoration of tensile properties; although weaker than 4W, drying had greater effect in the 4C3W specimen due to the protective outer layers of chopped mat; Figure 12. Conversely, 4C3W samples with higher resin content experienced lower modulus increase compared to the 11-month, saturated samples. In theory, complete restoration of properties can only be accomplished if there have been no irreversible changes to the resin through saturation. Additional damage such as fiber matrix debonding, microcracking, the onset of plasticization, and fiber damage may be observed during saturation resulting in greater strength loss.
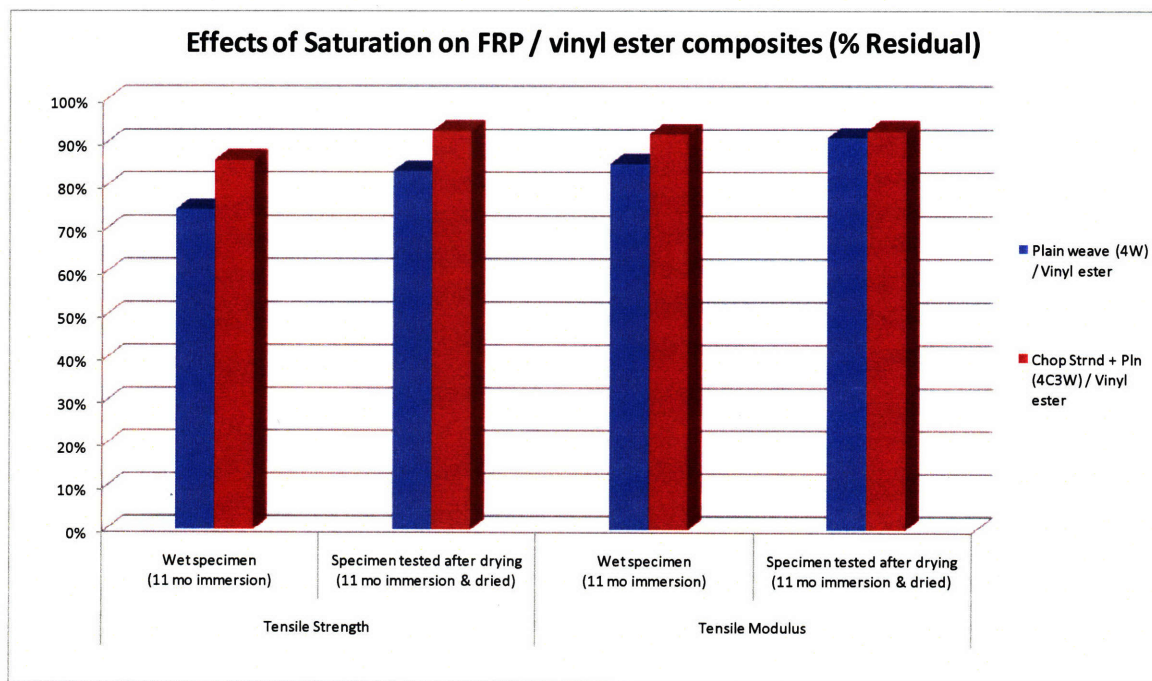
Figure 12: Effects of saturation on glass fiber / vinyl ester [50].

In addition to the tensile strength and modulus degradation, shear strength and material fatigue are affected by water absorption. A study of shear stresses between the adherend and glass fibers determined that fiber direction has the greatest effect due to the

existence of void spaces between fibers and the matrix; an effect compounded by water intrusion [46]. Figure 13 shows the normalized shear stress for woven mat, uni-directional, and bi-directional *glass / vinyl ester* composite samples immersed in 80°C distilled water relative to samples not subjected to the test environment. This experiment was conducted over a shorter time frame than the previously referenced works. Because of this, the unidirectional sample was found to absorb more water causing the matrix to swell, reducing the interfacial voids that would otherwise reduce the shear strength. High void content results in 1) weaker interfacial strength due to inadequate adhesion, 2) mutual abrasion of fiber, and 3) crack initiation and growth due to void colecense [27].
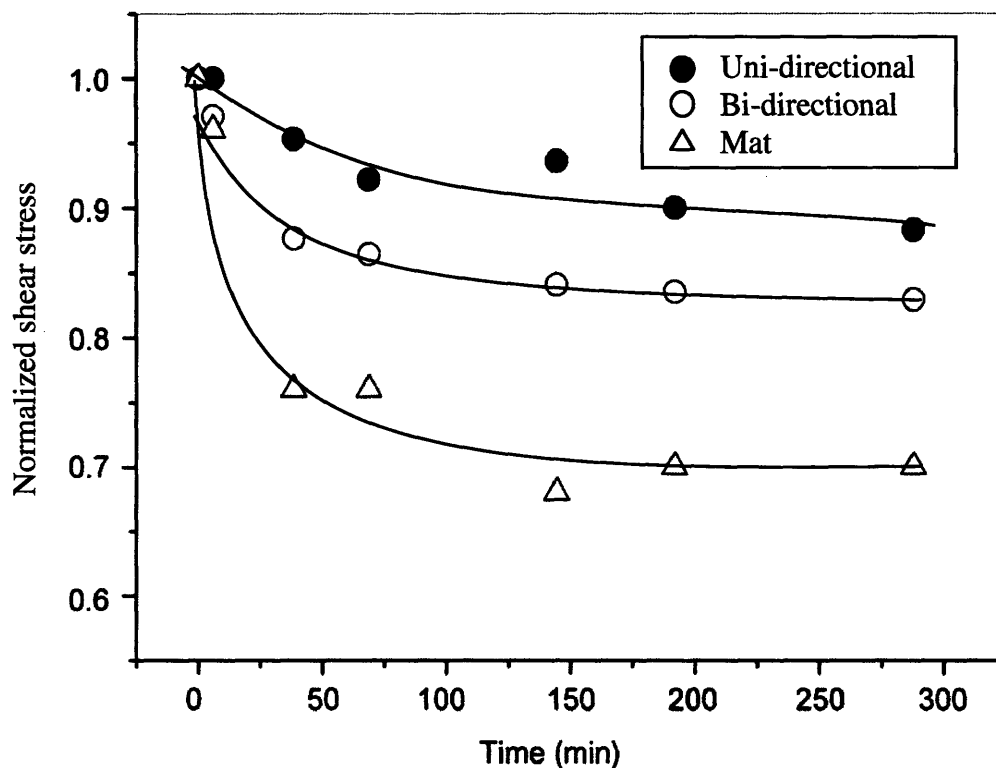
Figure 13: Resistance to shear stress during water immersion at 80°C [46].

In the marine environment, flexural strength is a primary concern for fatigue life whether the structure is part of underwater piping systems, ship's hull, or appendages. *Carbon* fiber laminate composites, plain woven and multi-axial, have been studied for

flexural and fatigue degradation under saturated conditions, 0.6% weight [53]. Figure 14, shows the difference between saturated and dry **carbon / vinyl ester** specimens after soaking in 95°C water for 120 hours and reaching saturation weight. While plain-woven specimens do not show appreciable differences, multi-axial fabrics, which likely have higher void content, display significant fatigue degradation over time compared to dry samples.
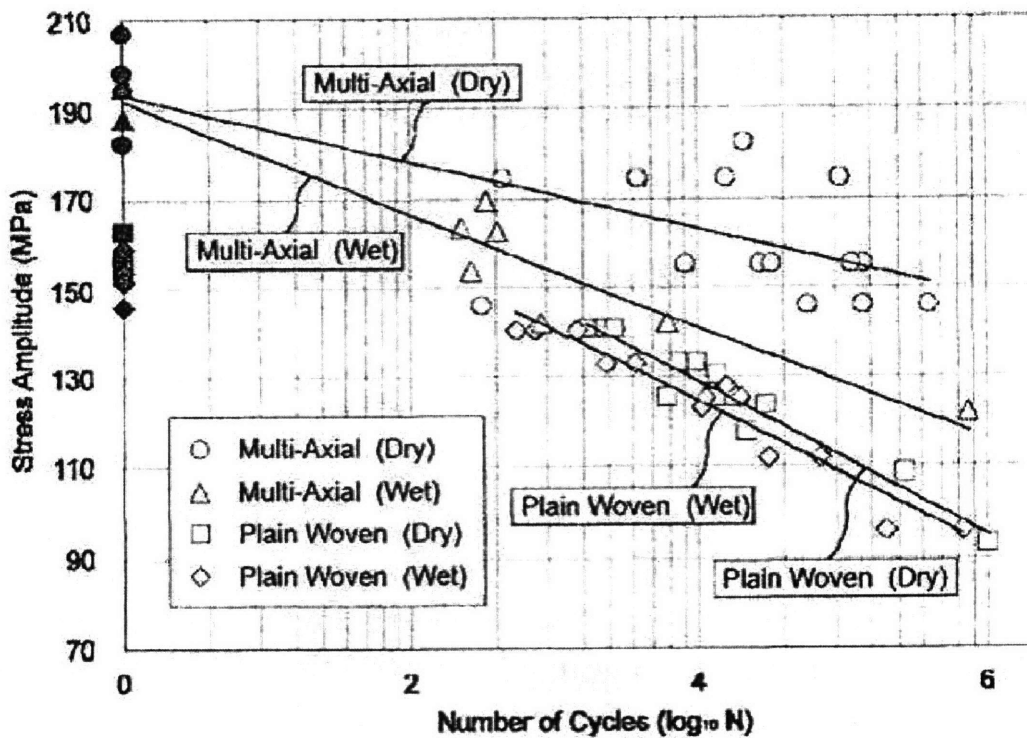
Figure 14: Fatigue strength comparison of saturated and dry CFRP laminates [53].

Additional research discovered chopped strand **glass** mat with **polyester** resin and **epoxy** resin subjected to marine environments including immersion in saltwater for up to 18 months [55]. Results show reduction in flexural strength of **polyester** laminates between 14 - 22% and 10 - 15% for **epoxy** laminates. Concurrent with other sources, this research states that some resins, including **vinyl ester**, have displayed up to 30% reductions in

flexural strength. *Polyester* laminates, however, immersed in seawater show impact strength reductions of up to 60% after 18 months.

3.3.1 Petroleum Products

Fuel-water immersion testing with JP-4 on *graphite (carbon) / epoxy* and *Kevlar / epoxy* resins reduced the tensile strengths by 11% and 25%, respectively [37]. Shear strength was reduced by as much as 40% in both materials (Figure 15). Similarly, General Motors tested *E-glass / polyester* and *E-glass / vinyl ester* in a high-temperature, moist environment with fluids including automotive brake fluid, saltwater, and diesel fuel. Though no numeric results were provided, the experiment discovered that saltwater, antifreeze, and gasoline have the most detrimental effect on composite strength.
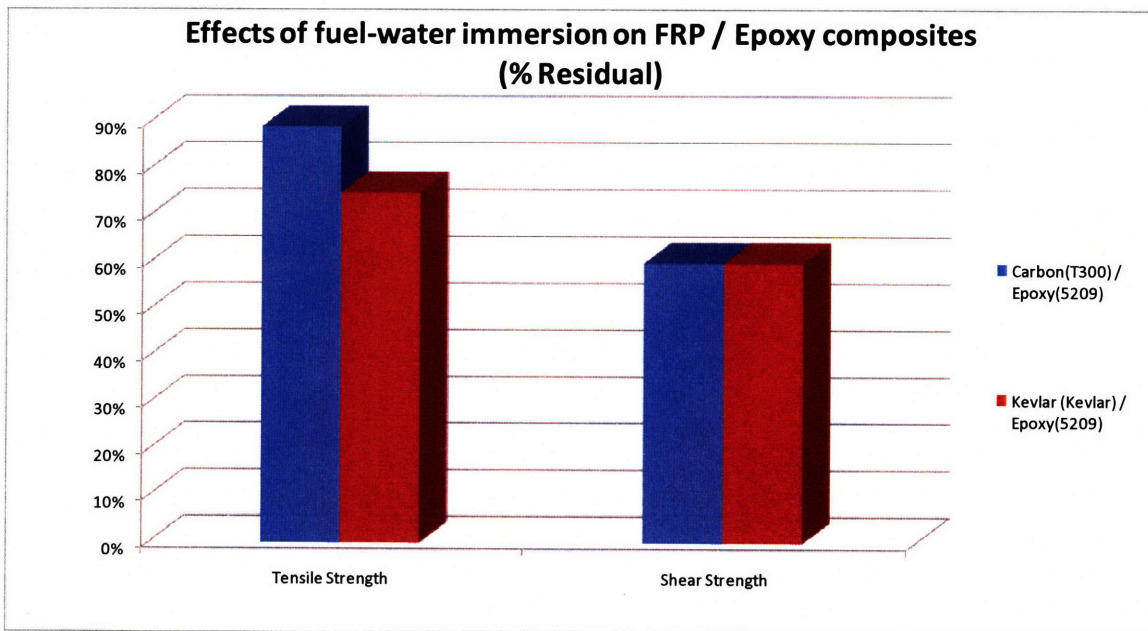
Figure 15: Effects of fuel-water immersion on FRP / epoxy [37].

3.3.2 American Bureau of Shipping Damage Assessment

The American Bureau of Shipping (ABS) states that in the event of moisture intrusion into the laminate hull structure, no repair is to be conducted until the part is rinsed with fresh water and allowed to dry for a minimum of 48 hours [45]. Additionally, laminate moisture content must be less than 0.5% by weight or less.

An increase in void content from 10% to 40% decreases flexural strength by a factor of three and reduces the elastic modulus by half. Therefore, detection and repair of voids caused by either delamination or manufacturing flaws must be considered before damage propagates to unrepairable levels [27]. ABS limits void content to less than 4% of the structure, and where void content is greater than 2%, requires additional testing [45].

3.4 Summary

The marine environment contains corrosive materials, fluids, and hazards capable of attacking composite materials. Through vigilant inspection techniques and assessments, proper repair levels can be determined. Figure 16 graphically illustrates the relationship between level of damage complexity, moisture absorption, and effective level of repair. In the absence of quantitative rules, prudent engineering knowledge must be applied to determine the level of repair or if a component should be scrapped. Referenced work provides evidence that moisture intrusion inhibits the use of permanent repair methods underwater. The use of materials specifically manufactured for underwater curing such as pre-preg composite mats or epoxies combined with pressure or vacuum treatment methods may offer the possibility of semi-permanent or temporary

repairs to specific components in the underwater environment until resources are available for permanent repairs or validation can be made for classification as permanent.
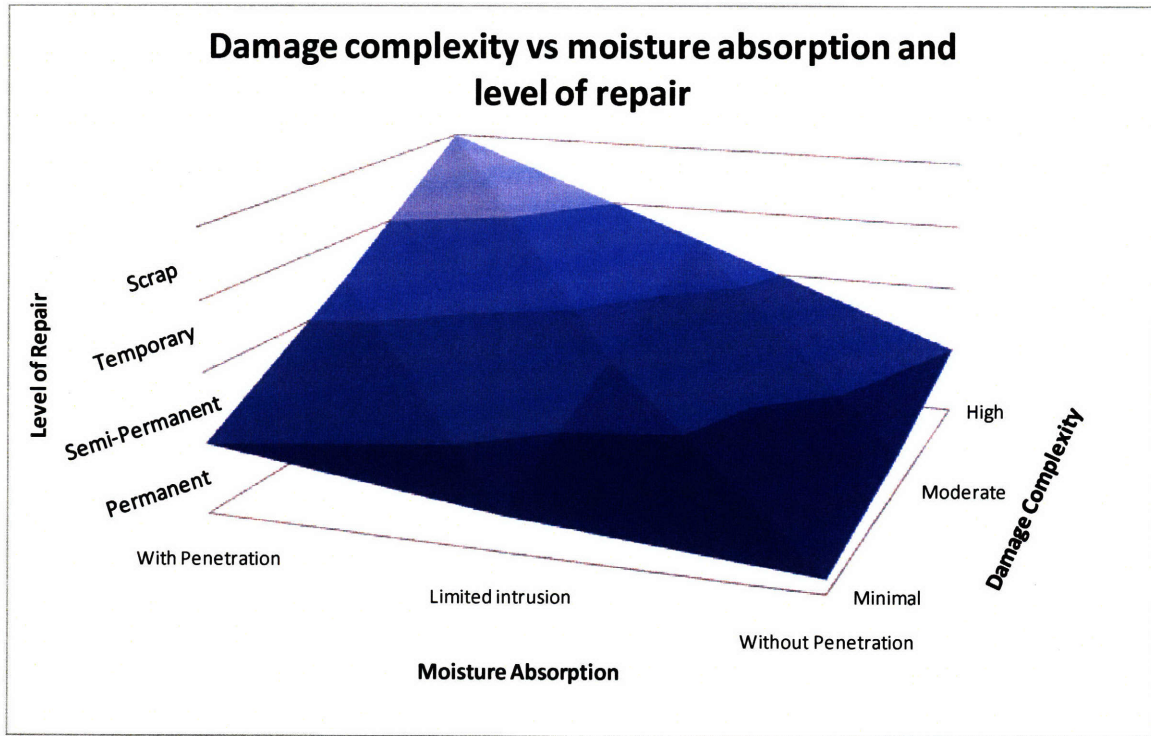
Figure 16: Schematic of damage complexity versus moisture absorption and level of repair.

4

COMPOSITE REPAIRS

4.1 Introduction

Composite repairs occur in many different forms throughout industries including aerospace, oil and gas, civil, and marine. However, there is limited speculation to applications underwater and even less actual data reviewing effectiveness of repairs performed underwater. Numerous factors affect material repairs including adhesive selection, bondline thickness, patch overlap, patch shape, taper, and scarf angle. While most factors have been briefly discussed in previous work by Panagiotidis [101], scarf angle, taper, surface treatments, and adhesive bonding will be revisited in conjunction with different repair types. Ultimately, material selection and careful repair of a composite structure may determine the difference between success and failure of the repaired structure.

4.2 Patch Design

Damaged composites, regardless of the damage assessment or cause should be repaired beginning with the removal of compromised laminates. Adhesive patch design plays an important role in the effectiveness of repairs and has the potential to eliminate stress concentrations caused by mechanically fastened joints [37]. Adhesive joints rely on several key design features for a successful joint: taper angle, patch adherend taper, spew fillet, adhesive bondline thickness, and surface preparation. In each case,

composite patch design seeks patch failure within the adherend rather than the adhesive [68].

4.2.1 Scarf Angle

One of the primary parameters of repair is the scarf angle, which is used to obtain higher bond strength between the adhesive, repair laminate, and original structure. Figure 17 and Figure 18 illustrate the differences in tapered scarf repair and tapered step repair, both of which are shown with a backup ply. Scarf tapered repairs are sanded with sloped surfaces by sanding at exact angles to remove discontinuities and achieve a uniform stress distribution throughout the repair [30]. Inconsistent angles may change the adhesive bondline thickness and result in strength loss and susceptibility to fatigue [25].

Step sanded repairs are more commonly used on *glass* fiber laminates than on stronger *carbon* fiber laminates where individual layers are more difficult to differentiate. Inadvertent cutting of adjacent layers can reduce or destroy that layer's strength and decrease the laminate's overall structural integrity, effectively undermining any benefit gained from the repair. Though contradicting arguments have been made concerning the simplicity of creating each type of repair, it is generally acknowledged that both types require skilled laborers and specialized tools [25, 30].
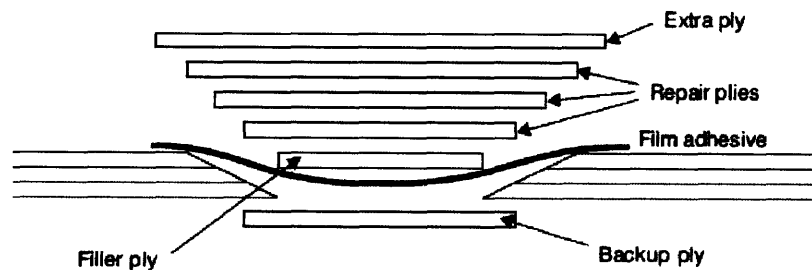
Figure 17: Scarf tapered repair [62].

Step repairs, similar to those shown in Figure 18, are most common on radomes or where radar transmission cannot have excess material that may interfere with radar permeability [25, 30]. As previously mentioned (Section 3.2.1), the carbon fiber superstructure of DDG-1000 will also require careful repair methods due to radar reflectivity. Repairs that are not uniformly smooth with the surrounding structure will increase the radar cross section of the vessel thus decreasing its' stealth capability and nullifying millions of dollars of research and development.
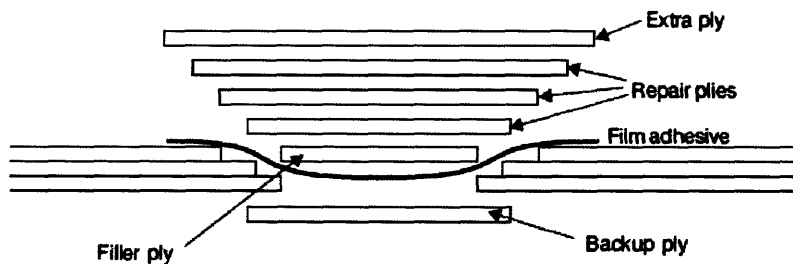
Figure 18: Step sanded repair [62].

Due to the extensive use of composites, specifically thin sandwich panels, the aerospace industry provides a wealth of information on repair methods and scarf repair angles. Repairs conducted on aerospace composite panels have been recommended by the Structural Repair Manual to have scarf angles between 2° and 6°, depending on the location and thickness. A 2° (1/50 slope) repair angle should be used on thinner structures, while a 6° (1/20 slope) taper is permitted at panel edges where thickness increases for bonding and stress reduction [25, 47, 49]. A high angle scarf repair presents several disadvantages when applied to thicker marine panels, the most prominent being removal of large quantities of undamaged composite laminate structure. For example, damage to a 10 mm thick marine panel, using a 1/50 scarf angle or 12.5 mm per step, requires removal of 500 mm of laminate from the suspected edge of damage (Figure 19), likely an excessive amount [47].
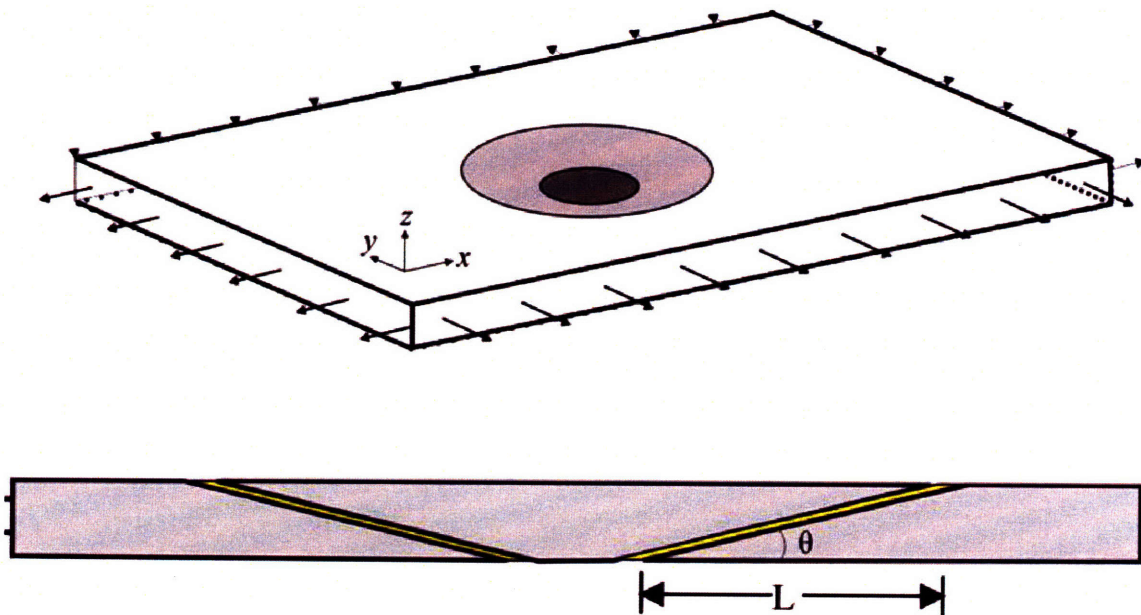
Figure 19: Scarf repair angle [49].

Ultimately, the balance between scarf angle or step angle and the maximum strength recovered should be optimized. Gama, et. al., conducted experiments with a 13.2 mm thick, 22-layer, S2-*glass* fabric plain weave / *epoxy* resin marine laminate [47]. Specimens were prepared using the Vacuum Assisted Resin Transfer Molding (VARTM) process, which produced a nominal fiber volume fraction of 50% and less than 1% void content. The experiments consisted of bending stiffness and percent renewed compressive strength after repair for three scarf repair angles: 45° (1/1 slope), 18.4° (1/3), and 11.3° (1/5).

Compared to a virgin specimen, elevated-temperature cure repair is capable of achieving 100% renewal of bending stiffness, while a room-temperature cure repair achieved 85% due to a lower adhesive modulus. It was also discovered that the bending moment at failure was highly dependent on the adhesive and scarf angle (Table 3). Testing of static strength versus scarf angle produced similar results, illustrating scarf angle importance. A 45° angle provided the least suitable results, and the 11.3° angle

resulted in the most promising strength renewal, up to 65% for both room temperature and elevated temperature cured adhesives. Figure 20 shows data collected for three scarf angles versus strength renewal as a percentage of the virgin compressive strength.

Table 3: Bending moment at failure [47].

| | Bending moment at failure / unit width (kN-m/m)[*] | | | |
	Hysol EA9359.3NA	Hysol EA9394	Plexus MA425	Plexus AO420
45° scarf (1/1)	1.97	1.65	1.13	0.95
18.4° scarf (1/3)	4.60	3.34	3.36	4.05
11.3° scarf (1/5)	5.49	3.83	5.91	5.44

[*] To be compared with bending moment at failure for control beams: 8.79 kN-m/m.
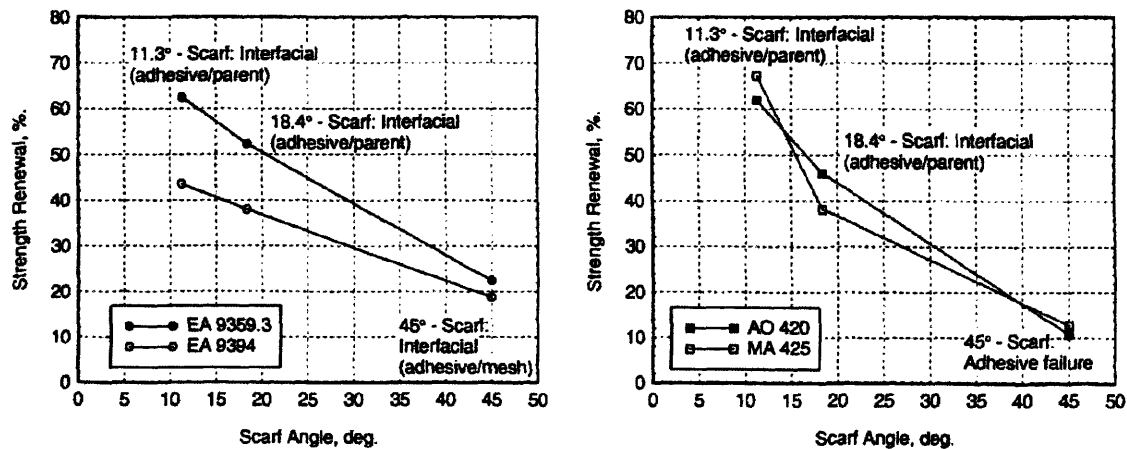
Figure 20: Repair strength renewal versus scarf angle [47].

Scarf Angle Optimization

Optimization of the scarf angle must consider both the adhesive and adherend design loads. Through mathematics and experimentation, Wang and Gunnion [49], showed that optimal scarf angle occurs when the maximum laminate tensile strength equals maximum adhesive strength. Through finite element analysis of a *carbon / epoxy* composite laminate, a predicted measure of repair efficiency was found to be 0.67.

Plotting efficiency against scarf angle, determined by equation (1) for a selected adhesive resulted in Figure 21.

$$\theta = \frac{1}{2}\sin^{-1}\left(\frac{2\tau_Y g(\gamma_{ult}/\gamma_Y)}{E\varepsilon_{DUS}}\right) \qquad (1)$$
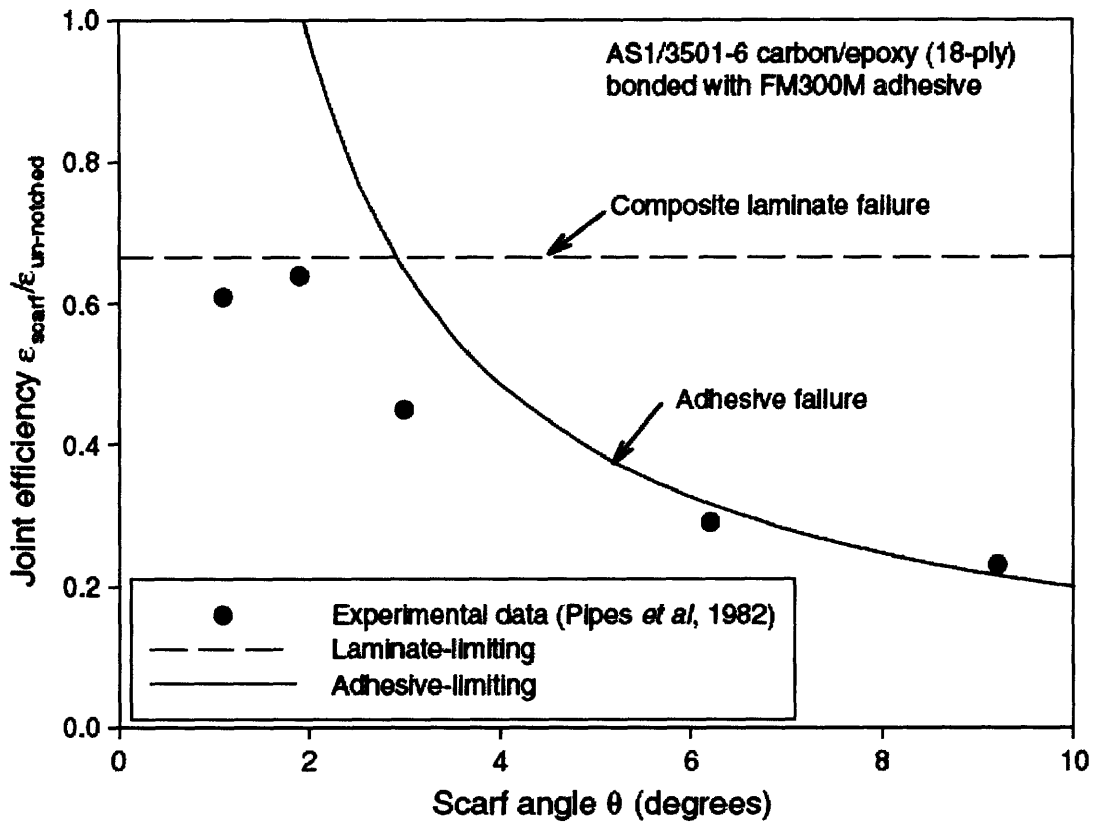
Figure 21: Optimized scarf angle: experimental & predicted [49].

Figure 21 illustrates the comparison of numerical results for *carbon / epoxy* laminates with experimental results produced by Pipes, et. al. [49]. For this particular composite and adhesive combination, the optimal angle was found to occur at 2.9°. Inspection of the graph shows a high correspondence between experimental data and finite element
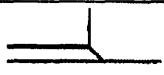
analysis. Consequently, the graph also illustrates the reduced joint efficiency as the scarf angle increases.

It should be noted that work referenced in Section 4.2.1 did not employ extra plies applied over the top or bottom of the repair. In practice, extra plies minimize peel stress and greatly decrease fatigue failure at the repair ends after long periods of time at high loads [25]. Although not addressed in this work, Panagiotidis [101] extrapolated data from other research showing tensile repair efficiency up to 96% strength renewal compared to virgin composite material.

4.2.2 Patch Taper

Patch taper addresses the shape of the patch adherend material that best alleviates stress concentrations at the extreme ends of the repair where peel stresses are greatest [30, 37]. Through proper adhesive selection and joint design, peel stress can be reduced to acceptable levels. Table 4 shows a selection of simple and complex single-lap joints with different patch taper designs and spew fillets tested for bonding between aluminum and *glass / polyester* FRP.

Table 4: Tapered joints for glass FRP bonded to aluminum [30].

Joint		Joint Strength (N/mm)	Failure Location
A		69	Adhesive
C		182	Adhesive
F		252	Adhesive
G		323	Adhesive
I		375	Metal & adhesive
K		375	Metal
L		375	Metal
M		375	Metal

In each case, evaluation of the tested designs identified the critical bond and the joint strength at failure.

As the joint configurations in Table 4 become more complex and transfer the stresses from the tip to the underlying structure, the joint is capable of higher bond strength. Conversely, the lowest joint strength occurred with the removal of the fillet causing a high stress concentration, which corresponds with the notion that removal of the spew fillet decreases the durability of the adhesive bond [56].

Table 5 was constructed with *glass* fiber chopped strand mat / *polyester* resin and shows much lower critical bond strengths. Incidentally, failure occurred at the adhesive / composite bond rather than the base material as with pultruded *glass* / *polyester* regardless of the taper shape.

Table 5: Chopped strand mat glass fiber / polyester [30].
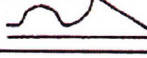
Joint		Joint Strength (N/mm)	Failure Location
C		78	FRP
F		102	FRP
G		144	FRP
J		134	FRP
K		135	FRP
N		135	FRP
O		135	FRP

Figure 22 shows a direct comparison of joint strength at failure between the chopped strand mat and pultruded glass fiber samples with differing lap joint configurations.
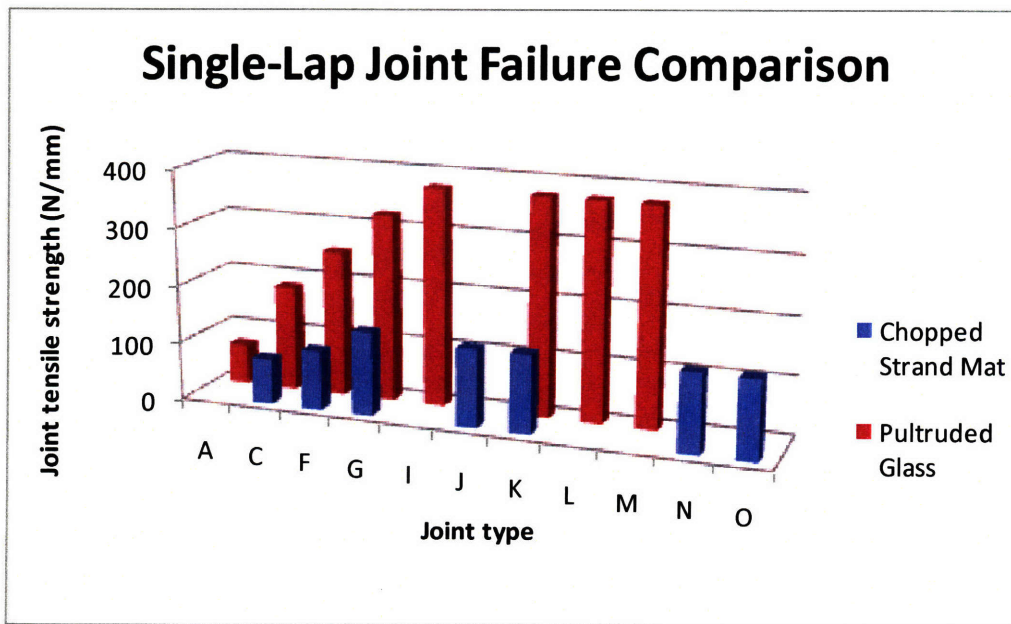
Figure 22: Single-lap joint failure comparison [30].

Single-lap joints, by themselves, even with uniformly thick adherends, are the most inefficient joint type and are the most susceptible to failure through bending loads [37]. Thus, addition of spew fillets and a combination of scarf patches, single-lap joints, and proper adhesives must be determined.

4.2.3 Spew Fillet

Spew fillet is the excessive adhesive material pressed beyond the boundaries of the patch during the repair process, providing additional stress distribution [44]. Research suggests that a spew fillet may reduce peel stress by more than 32% [68]. The variations of spew fillet geometry and associated stresses clearly illustrate the spew fillet's advantage [58]. Further analysis compares three different evaluation methods, including finite element and theory for adhesively bonded aluminum plates. These analyses modeled a 45° spew fillet twice the thickness of the adhesive [$(h_{sp}/h_a)=2$] as shown in Figure 23 [58].
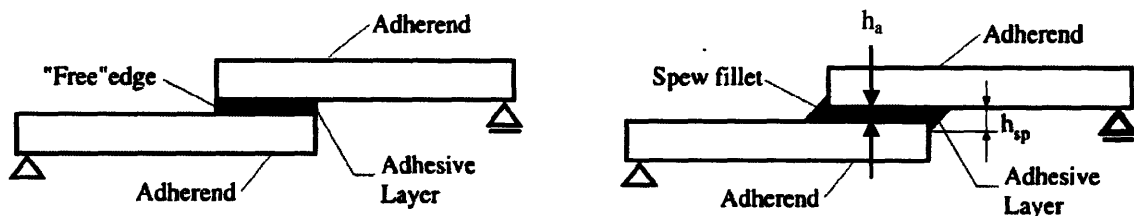
Figure 23: Adhesive bond wihout and with spew fillet [58].

Figure 24 shows a maximum peel stress of slightly more than 0.82, while Figure 25, an example without a spew fillet, is more than three times that factor. In both figures, the stresses are normalized by the adhesive strength. Thus, a joint without a spew fillet would be structurally weak and very susceptible to fatigue and failure [58].
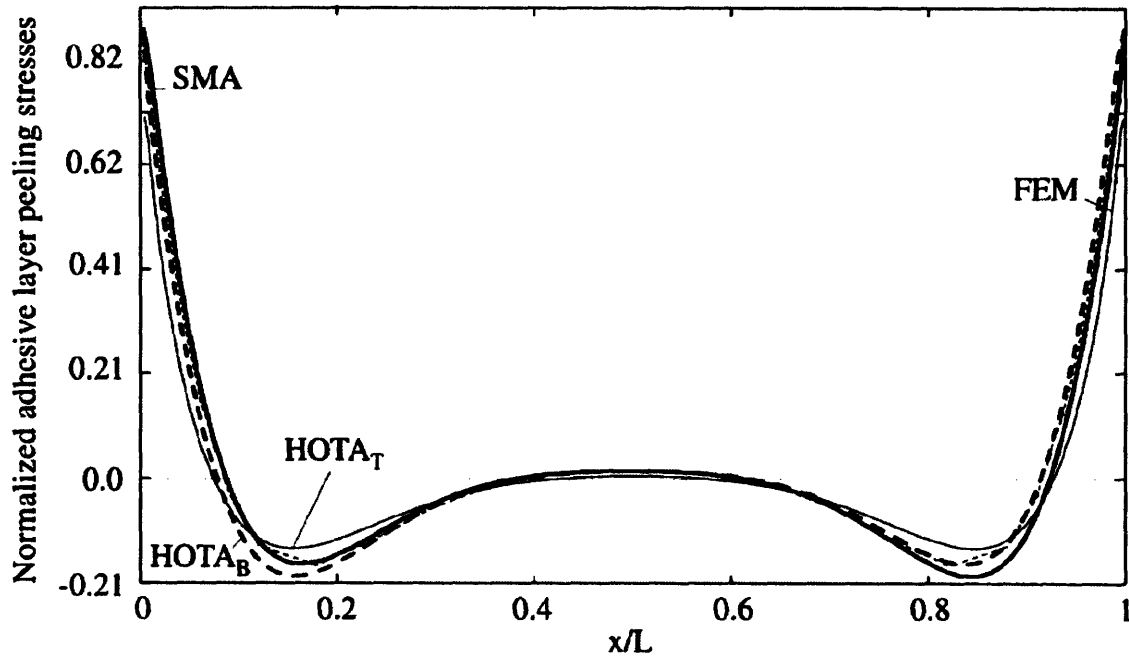
Figure 24: Bondline peel stress with 45° fillet (2x adhesive thickness) for a joint of length (L) [58].

(SMA: Spring model approach; HOTA: High order theory approach; FEM: Finite element method)
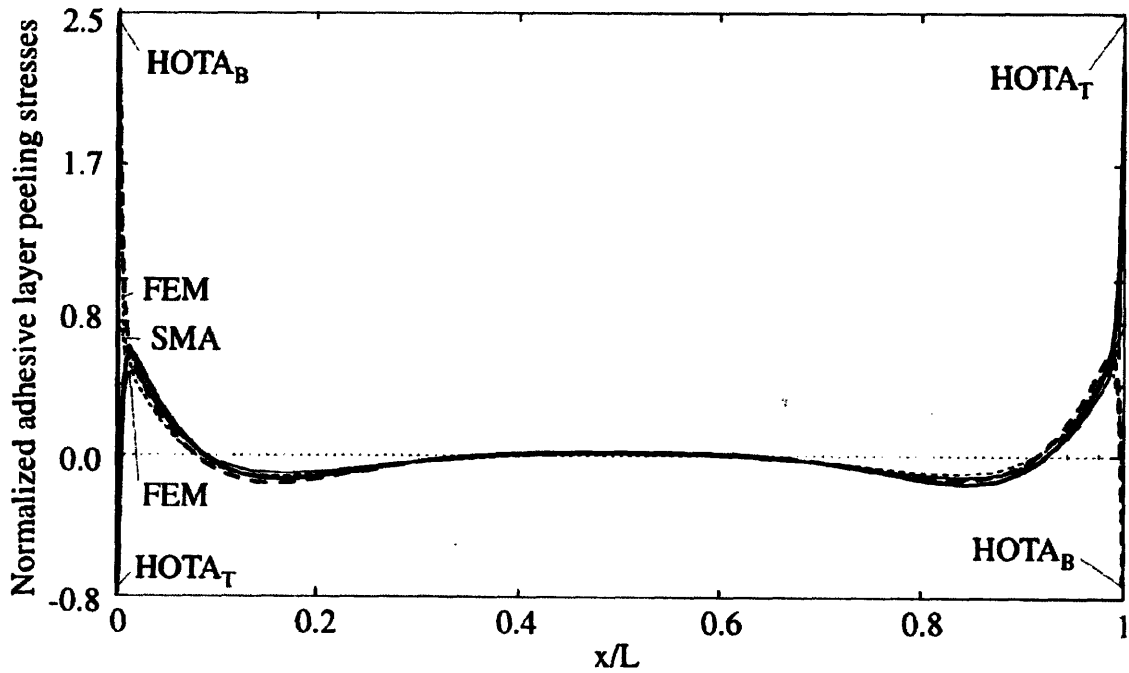
Figure 25: Bondline peel stress without fillet for joint of length (L) [58].

(SMA: Spring model approach; HOTA: High order theory approach; FEM: Finite element method)

4.2.4 Bondline Thickness

Single-lap repair patches may be subjected to large stresses and cyclic loading, which are transmitted through the adhesive bonding layer between the patch and adherend. In all patch designs, the common goal is to provide an adhesive bond that transmits stress to the adherends and fails within the adherend near the adherend/adhesive interface prior to adhesive failure [37]. Excessively thin adhesive layers and corresponding patches may present undesired flexibility or weakness [30, 60, 61]. However, thicker patches create overly stiff structures that result in increased brittleness and added weight. Figure 26 and Figure 27 illustrate the relationship between adhesive bondline thickness and the resulting failure stress.
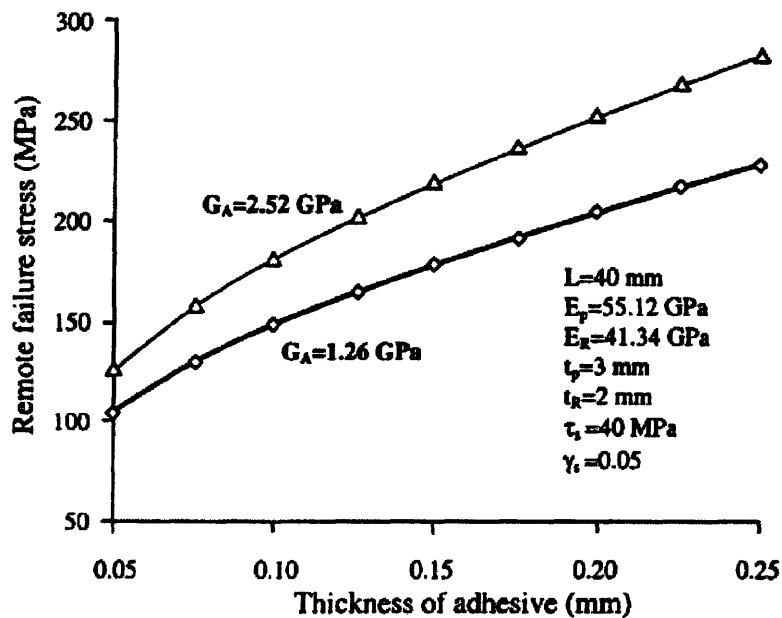
Figure 26: Failure stress versus adhesive thickness [60].
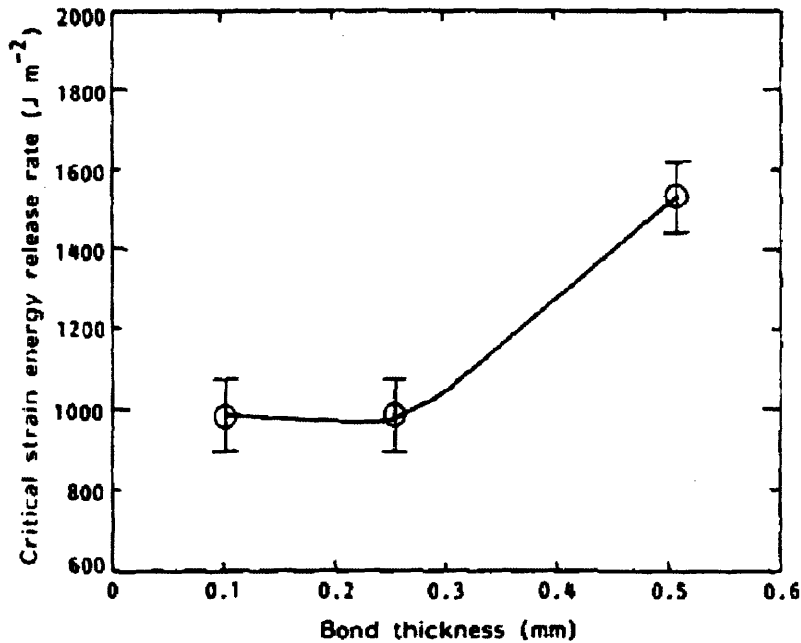
Figure 27: Critical failure energy versus thickness [61].

Additionally, Figure 28 illustrates the relationship between adhesive thickness at the end of the patch and a reduction in shear strain. As thickness increases, shear strain is distributed throughout the edge area resulting in a lower peak at the zero point. Therefore, a patch with an internal taper similar to taper 'G' in Table 5 combined with an appropriate adhesive thickness will substantially reduce the peel stress at the edge.
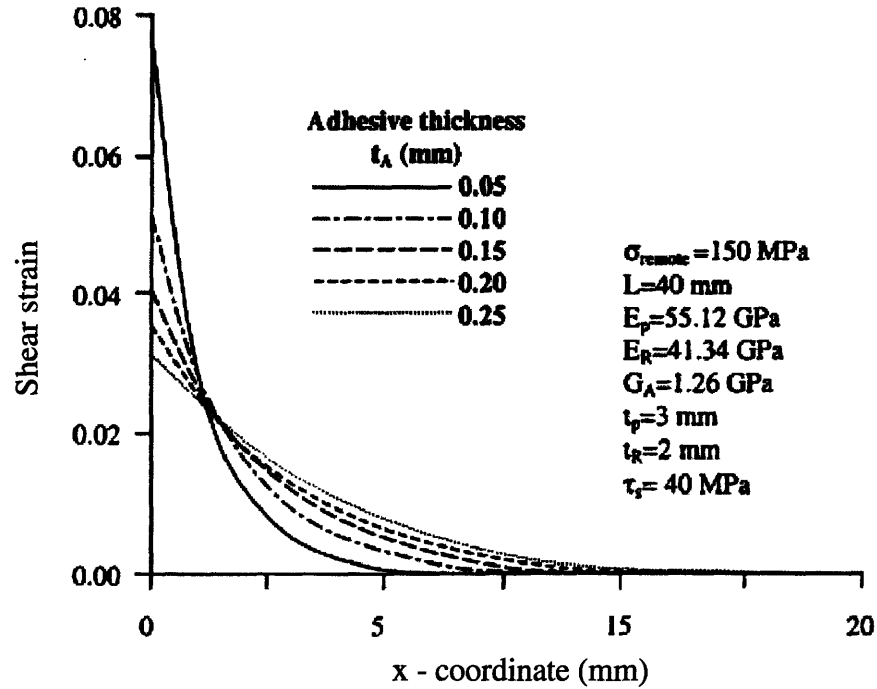
Figure 28: Patch end shear strain versus adhesive thickness [60].

Further analysis concerning bondline thickness for single-lap joints in marine FRP structures is shown in Figure 29 [30]. Four different flexible polyurethane adhesives were compared and produced data showing relatively little improvement in yield strength and, in three cases, degraded effects above 4 mm adhesive bondline thickness. Ultimate strength, shown in Figure 30, displayed similar results; however, two adhesive specimens, though much stronger, showed drastically reduced performance above 1 mm adhesive bondline thickness. Other research suggests that increasing the thickness of the adhesive layer may reduce the stress concentration level by as much as 21% [68]. Thus, because of manufacturing and environmental variations, bond layer thickness is recommended to fall within the range of 0.125 – 0.39 mm for most joint types [37].
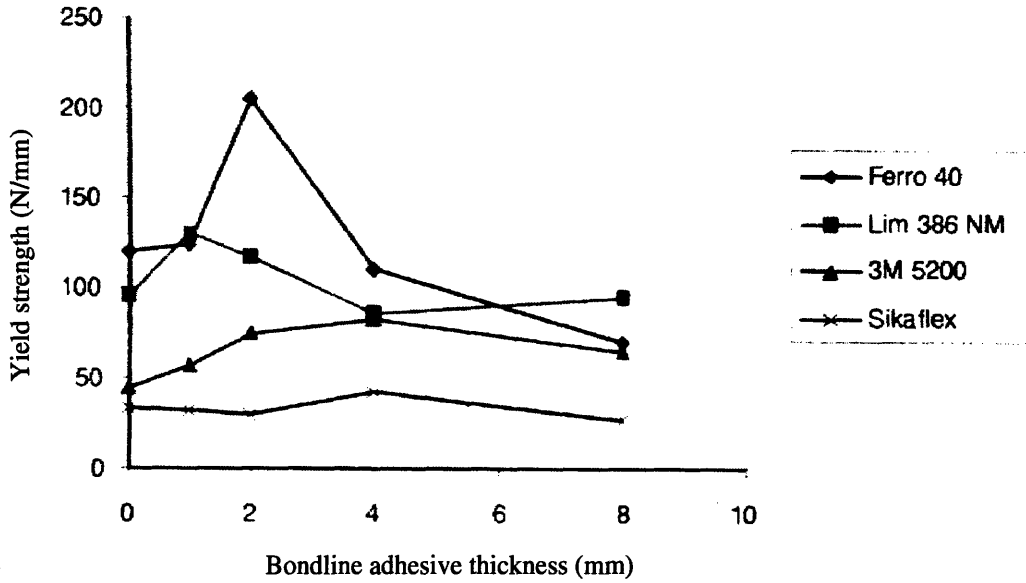
Figure 29: Single-lap joint bondline thickness versus strength [30].
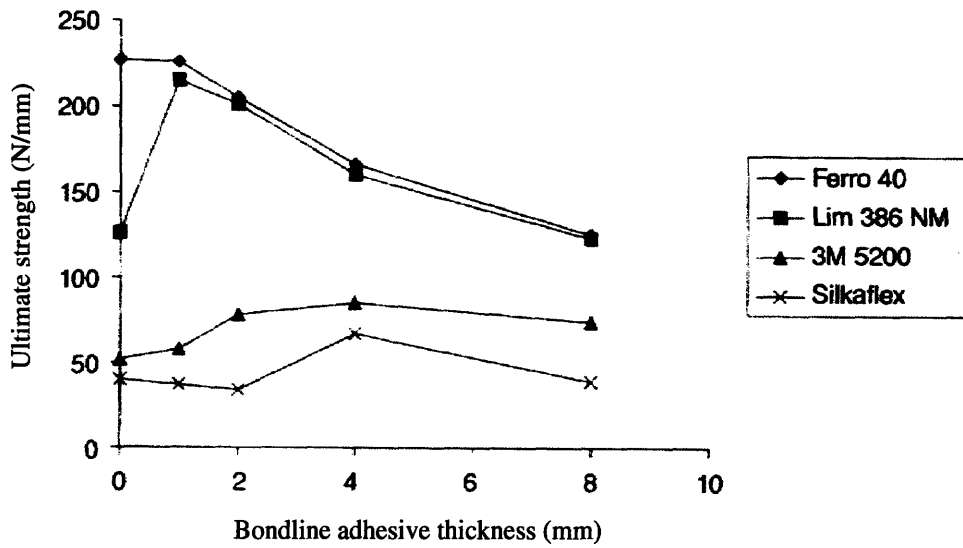
Figure 30: Single-lap joint bondline thickness versus ultimate strength [30].

4.2.5 Patch Overlap

Patch overlap refers to the amount of patch material extending beyond the known damage boundaries. Hu and Soutis [60] addressed the use of a circular double-lap joint patch over a hole representing damage removal from a structural laminate composite. Figure 31 was produced through the use of different patches with various thicknesses. With patch stiffness ($E_R T_R$) equal to twice that of the parent ($E_p t_p$) laminate structure, $E_R T_R / E_p t_p = 0.5$, and expected failure stress for a double-lap joint, the optimal patch overlap correlates to a length of 12 mm.

Considering the repair environment, procedures, and the multiple factors that affect the integrity of adhesion and material structure, as a rule of thumb, most patches should be extended to a length equal to 30 times the thickness of the adherend; particularly for single sided repairs, single-lap joints, or inhomogeneous composite laminate structures [44, 60]. While increased stiffness is a by-product of extended overlap length, additional consideration should be given to the repaired structure's intended purpose, as more structure includes more weight, but also increased load capacity.

Remote failure stress (MPa)

200

160

120

80

40

0

$E_R t_R/E_p t_p = 0.25$
$E_R t_R/E_p t_p = 0.5$
$E_R t_R/E_p t_p = 1$
$E_R t_R/E_p t_p = 2$

$E_p = 55.12$ GPa
$G_A = 1.26$ GPa
$t_p = 3$ mm
$t_A = 0.1$ mm
$\tau_s = 40$ MPa
$\gamma_s = 0.05$

0   5   10   15   20   25   30   35   40
Bonding length (mm)
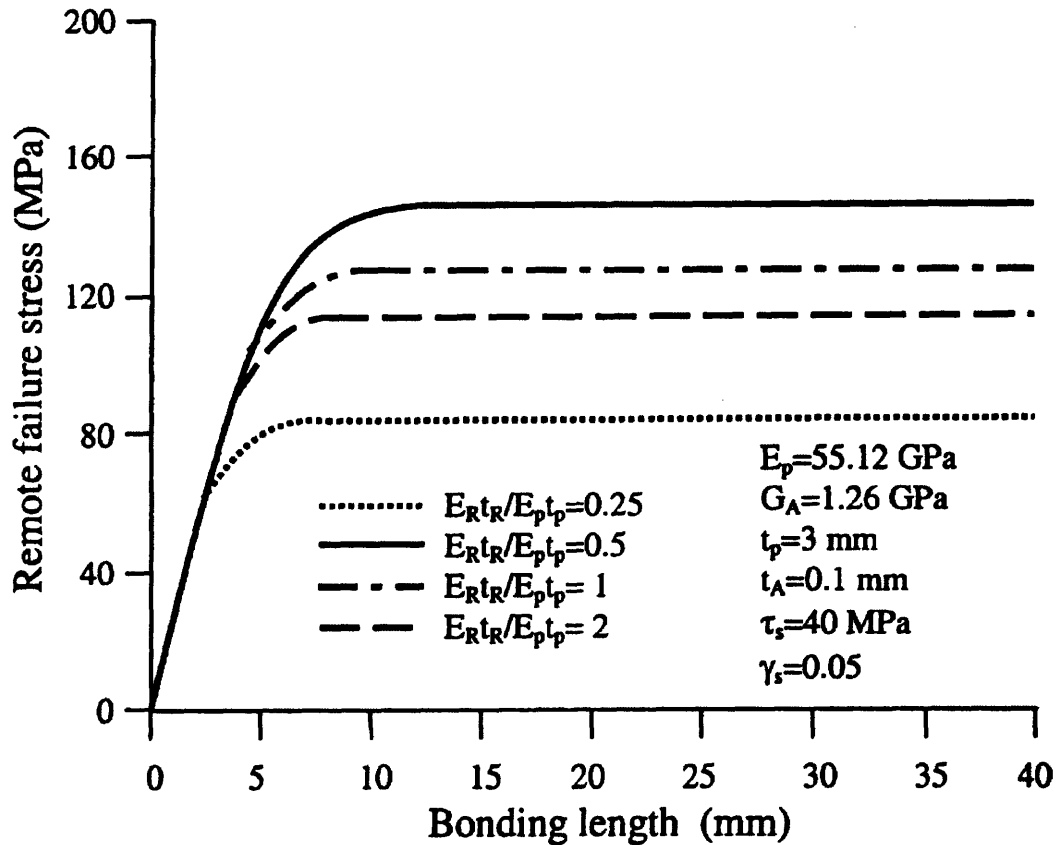
Figure 31: Failure stress of double-lap joint versus bond length [60].

4.2.6 Surface Treatment & Adhesive Bonding

Repair failures are most likely to occur after aging of the adhesive / adherend interface [56, 68, 71]. Surface preparation focuses on the steps taken to improve adhesion for increased strength and resistance to environmental effects after the damaged or weakened structure has been removed. Structural bonding of two components through adhesion can be accomplished with a combination of mechanical interlocking and chemically bonding polymer molecules to the composite structure [56, 57]. Experience has shown that pre-bond surface preparation through surface roughing that eliminates smooth surfaces and removes contaminants that would otherwise prevent adhesion can significantly improve strength and durability of adhesive joints.

The use of surface primers has been well documented for a number of materials, including metal-to-composite and composite-to-composite bonds. Primers, such as silane, enhance bonding by displacing water molecules and removing microscopic particles that prohibit adequate bond contact. Table 6 reveals data concerning the exposure of single-lap joints between steel panels at 100% humidity, illustrating the importance of an appropriate surface treatment to extend the time to failure of a specimen under stress and the reduction in lifespan as load increases. Additionally, Figure 32 provides data for similar steel specimens in which silane primer samples were approximately as effective as the proprietary products after prolonged exposure [30].

Table 6: Time to failure, 100% humidity [30].

Surface Treatment	Load (kN)	Time to failure of triplicate specimens (days)		
Degreased	0.4	72	86	86
	1.0	44	44	44
	2.0	25	28	28
Oiled	0.4	62	66	70
	1.0	24	25	25
	2.0	0	0	0
Accomet C (proprietary)	0.4	254	>1121	>1121
	1.0	89	103	110
	2.0	18	18	19
Silane coupling agent GPMS	0.4	>1121	>1121	>1121
	1.0	124	126	128
	2.0	26	28	28
EP 2005 (proprietary)	0.4	96	99	125
	1.0	62	63	64
	2.0	12	12	12
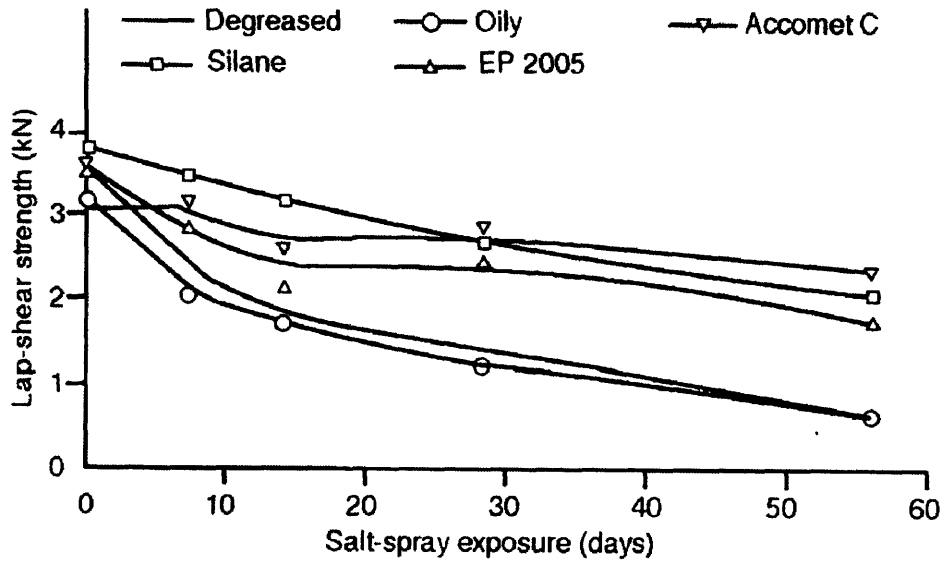
Figure 32: Effect of salt spray correlated to preparation methods [30].

Surface preparation, as mentioned, also includes roughening the surface of the adherends, which creates a larger effective bonding area for the adhesive [30, 57]. Several methods exist to accomplish surface roughening: sanding, grit blasting, and chemical etching. While sanding and chemical etching are both plausible methods; time, accuracy, and safety are primary concerns with either process. When sanding laminates, caution must be used to avoid penetrating layers or creating uneven surfaces. Chemical abrasives used to etch metals can also be caustic to the material as well as to personnel. Alternatively, grit blasting has been used extensively on metal and composite laminates for clean and uniform surface preparation in high strength bond applications and is the most reliable method [37, 57].

The combined effects of surface roughening and surface treatments are illustrated in Figure 33 and Figure 34 [30]. Experimental data are provided for single-lap joints made with 3-mm *chopped strand mat (glass) / polyester* and *carbon fiber / epoxy* laminate samples bonded to aluminum panels. In each case, the bond strength was significantly increased over specimens without surface treatment or simple sanding. Grit

blasting and grit blasting plus chemical etching have the most pronounced effects, achieving nearly 60% relative to the highest achieved value [30, 71].
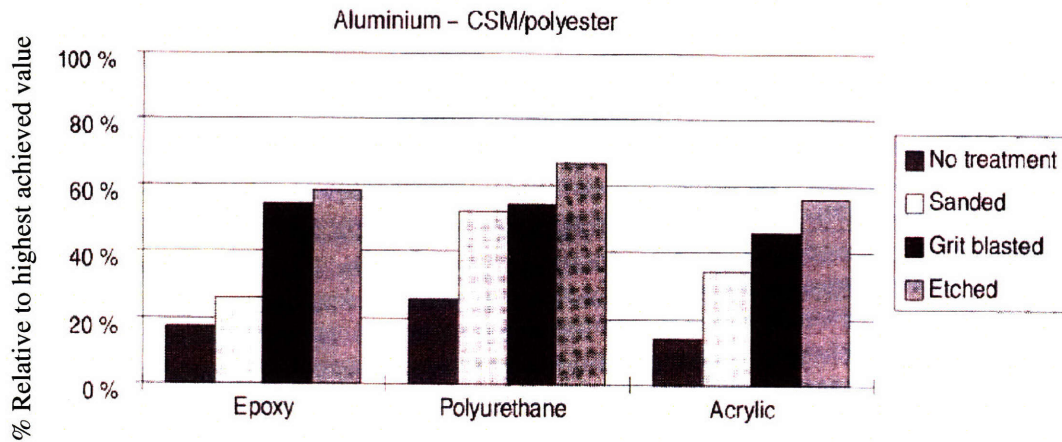
Figure 33: Aluminum-CSM/polyester surface treatments and adhesives [30].
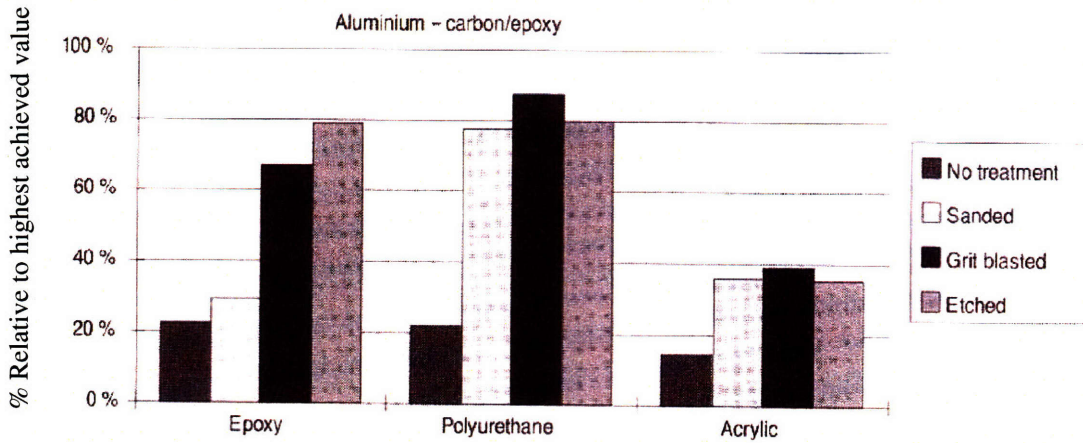
Figure 34: Aluminum-carbon/epoxy surface treatments and adhesives [30].

Additional experiments conducted with ***chopped strand mat (glass) / polyester*** and ***carbon fiber / epoxy*** laminate samples bonded to stainless steel panels produced similar data, Figure 35 and Figure 36 [30]. Again, experimental data show the benefit of grit blasting combined with polyurethane adhesive for high bonding strength.
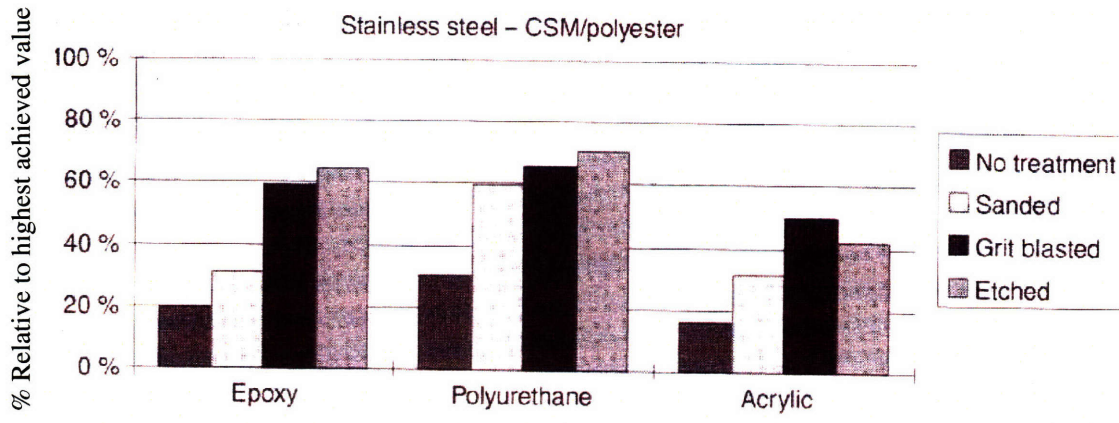
Figure 35: Steel -CSM/polyester single-lap joint surface treatments and adhesives [30].
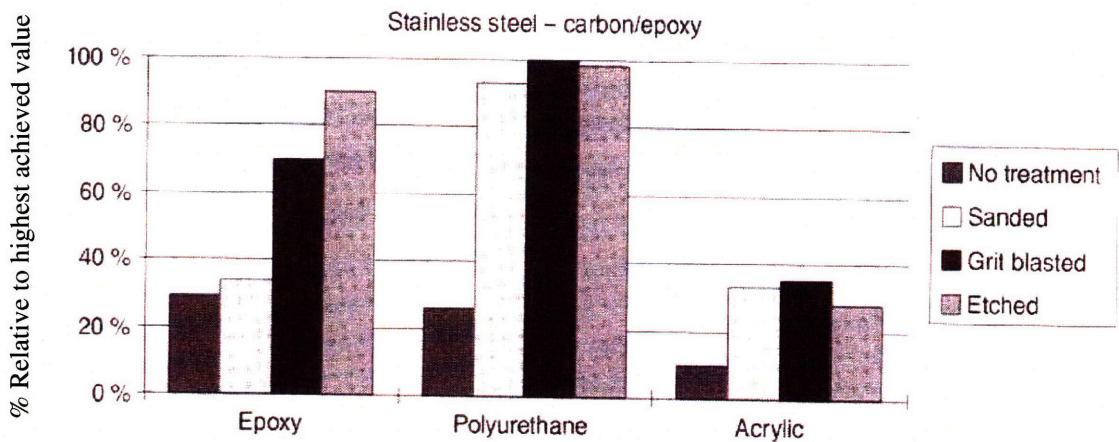
Figure 36: Steel-carbon/epoxy single-lap joint surface treatments and adhesives [30].

4.3 Composite Repair

Repairs can be completed in many different fashions, especially when dealing with emergency ship repair or marine salvage operations. Specifically, use of epoxies, steels, and composites has come into play during salvage engineering. In order to address and more thoroughly understand the materials available to the engineers and divers, we must comprehend the characteristics, strengths, and weaknesses of each in the underwater environment.

4.3.1 Steel versus Composite Materials for Marine Applications

Composite materials have grown in popularity with the marine industry over the last 50 years. Table 7 provides reasons for this increased interest in composites versus steel construction for small to medium size vessels [3]. Primary factors include weight reduction, corrosion resistance, low thermal and electrical conductivity, and low cost [65, 68]. Weight reduction has the added benefit of reducing hydrodynamic resistance, power required, and increasing stability through reduction of weight above the waterline. Thermal and electrical conductivity make composites adaptable to special applications including marine engine insulation and mine countermeasure vessels, which rely on reduced magnetic signatures for operation.

Table 7: Summary of differences between steel and composite construction [3].

Property	Steel Construction	Composite Construction
Weight	High	Allows significant reduction in structural weight
Corrosion	Rusts in marine environment resulting in high maintenance cost	Very durable in marine environment, little maintenance
Combustibility	Non-combustible, will not contribute to fire or generate toxic fumes	Combustible, surface must be protected in fire hazard areas
Thermal Conductivity	High, must be insulated to prevent fire propagation and to control infrared signature	Low, inherent insulation more than sufficient
Electrical Conductivity	High, inherently provides electromagnetic shielding	Low, must embed conductive layer if electromagnetic shielding is needed

Corrosion resistance is perhaps the greatest benefit for marine structures in the harsh saltwater environment. Even though, *carbon* fibers have been known to be susceptible to galvanic corrosion, *glass* fibers are virtually immune to the corrosive

effects of saltwater [68]. Additionally, FRP materials, especially sandwich structures, have pronounced shock-absorbing capabilities, more so than wood or steel.

Repair of high-strength *carbon* composites has been accomplished with the use of a single layer *glass* fiber lamina when contact with steel is necessary [68]. This adaptation provides an insulating layer between dissimilar carbon compounds that would otherwise cause an electrolytic reaction. Table 8 provides a comparison of *E-glass / vinyl ester*, *carbon fiber / vinyl ester*, and steel commonly used in marine applications and repairs [65]. Corresponding strengths and moduli are shown, depending on the material and manufacture. For example, the woven roving mat provides excellent strength in tension due to fiber weave. However, woven or bent fibers posses comparatively low compressive characteristics caused by stress concentrations as the yarns cross over in the weave pattern. These differences in mat construction have a direct effect on the fiber volume content, which is measured as a percentage of weight. According to the American Bureau of Shipping, marine composite laminate construction requires a minimum of 35% fiber content by weight [45].

In order to combat low compressive strength, stitch-bonded fabrics have been developed with only minor tensile strength reduction, which may be overcome with the use of additional layers of stitch-bonded fabric [65]. Stitch-bonded fabrics reduce the effect of misaligned fibers, the primary factor in reducing compressive strength by as much as 20%. Additionally, because of their construction, stitch bonded fabrics have excellent tear resistance, reduced manual labor during construction, less waste, and lower cost.

Table 8: Marine FRP strength compared to steel [65].

Properties		Direction of Force Application	E-glass woven roving	E-Glass Stich Bonded	Carbon Fiber Stich Bonded	Steel
Tension	Strength (MPa/g/cc)	Warp	259	196	717	64
		Fill	177	172	660	
	Modulus (GPa/g/cc)	Warp	15	12	36	24
		Fill	12	11	36	
Compression	Strength (MPa/g/cc)	Warp	184	238	286	64
		Fill	170	213	247	
	Modulus (GPa/g/cc)	Warp	16	13	43	24
		Fill	14	12	38	

4.3.2 Underwater Repair Issues

Following an adequate damage assessment, repairs, temporary or permanent, begin with the prevention of further moisture intrusion and the removal of chemicals, biological fouling agents, and petroleum products that may prohibit adhesive bonding between laminate layers and repair plies. In a dry environment, this may be accomplished through surface cleaning and either vacuum bagging or heating, or a combination of the two. However, the underwater environment presents a major challenge to composite repairs. Typical environmental solutions include the construction of a cofferdam that provides a dry habitat in which a diver works; still with the advent of underwater curing epoxies and resins, underwater repairs may be feasible.

Composite manufacturing methods include the use of hand lay-up or spray lay-up combined with the application of pressure to obtain higher fiber volume content. Hand lay-up may be used with mat fibers, while spray lay-up pertains to short fibers that are sprayed onto a mould or existing structure. Underwater application of spray type fiber composites will be impossible; however, pre-preg and wet lay-up composite fiber mats have been engineered for underwater applications. The term pre-preg applies to layers of fabric, woven *glass* or *carbon* fibers, impregnated with partially cured resin that will completely cure when exposed to a specific environment [3, 67]. Wet lay-up describes a

system that requires mat fiber impregnation on-site, immediately preceding application to the work piece.

Vacuum assisted resin transfer molding (VARTM), shown in Figure 37, has been used to achieve greater laminate compaction [3]. Similarly, SCRIMP (Seeman Composite Resin Infusion Molding Process) has been used to construct pilings and entire ship scale sections [69]. Both methods are capable of reducing voids and emission of solvent vapors during manufacturing.
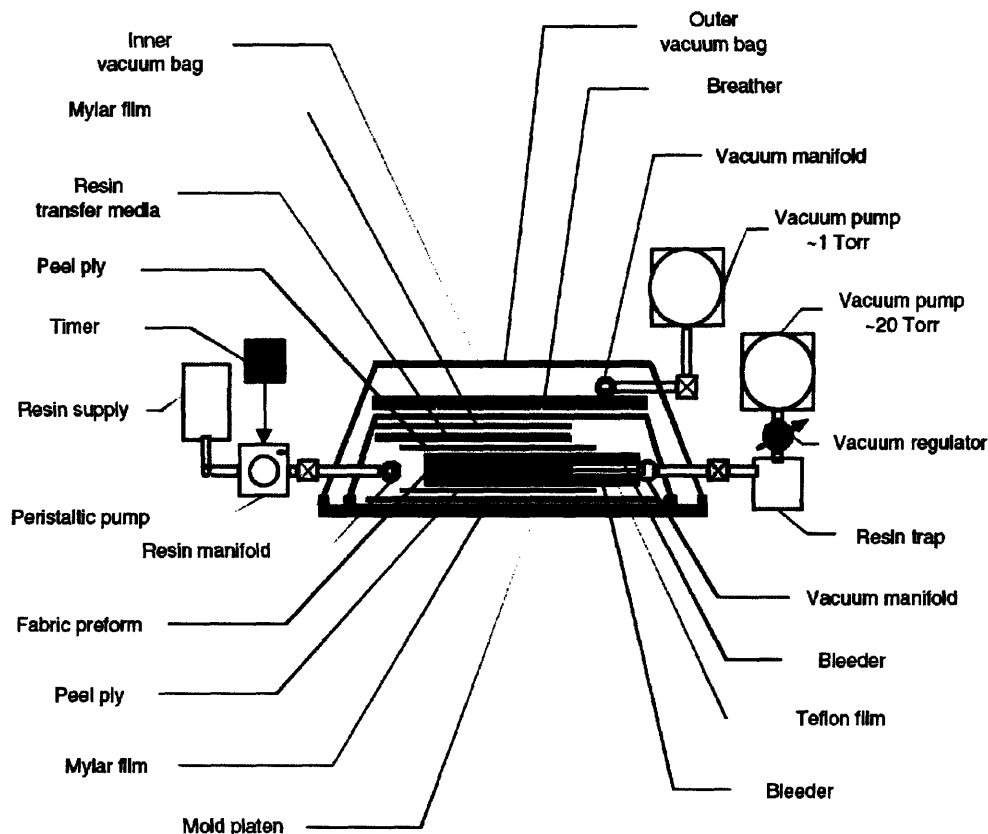
Figure 37: Vacuum assisted resin transfer molding (VARTM) configuration [65].

Modified underwater apparatus similar to VARTM and SCRIMP have been devised and patented to replicate conditions for bridge pile repairs [64]. Research conducted by the University of South Florida provided a system capable of applying

either a vacuum or pressure to the FRP wrap around a circular structure, resulting in the removal of water that may interfere with adhesive bonding.

In addition to environmental factors, repair types, and increasing the effectiveness of procedures, surface preparation in the marine environment is also important. This implies removal of marine growth and rough or sharp edges on the surface that may cause stress concentrations as fibers bend or fold over surface imperfections. On bridge piles, it was found that corners rounded to a radius of less than 19mm (¾ inch) yielded suitable results [67].

4.4 Summary

Composite repairs have particular tolerances for repair schemes and factors that contribute to the success or failure of the repair. The factors previously discussed include scarf angle, lap joint taper, spew fillet, bondline thickness, patch overlap, and surface preparation. Repairs should generally be performed after damaged material is removed with a scarf angle of 2° to 11.3°. Grit blasting surface preparation has proved to be the most reliable method for creating a uniform surface with proper bonding strength. Once the scarf patch is in place, a single-lap joint can be applied over the repair with a proper end taper and spew fillet for an acceptable stress distribution. The bondline thickness should be between 0.125 and 0.39 mm for a patch with an overlap 30 times the adherend thickness.

UNDERWATER REPAIR APPLICATIONS

5.1 Introduction: Underwater FRP and Epoxies

The last several years have seen an outreach to composite materials as they bridge the gap between traditional uses and more experimental applications. One experimental application is the repair of bridge piles, the vertical supports for the road deck, which are subjected to loadings, including wave action, corrosion, freezing water, and mechanical stresses. These loads act on the piles, resulting in concrete spalling and cracking throughout the piles with damage concentration at or just below the waterline.

Concrete repair methods are numerous from the more complex cofferdam systems similar to those used in piling construction to epoxy systems. Recent developments in underwater composite materials have provided non-toxic, simple to use systems requiring little or no technical training prior to installation and do not contaminate the environment. These improvements nearly eliminate the use of expensive and complex cofferdams and highly technical personnel required to perform the repairs.

5.2 Underwater Bridge Pile and Pipe Repair

Evidence suggests effective repairs can be accomplished underwater as demonstrated by repairs completed on bridge piles to restore structural strength and prevent future corrosion damage caused in the marine environment. Two examples have been thoroughly documented on bridge piles in a saltwater environment, while the open

literature revealed only one example of testing the bond strength of composites to steel pipes in a laboratory environment as would be observed in the oil and gas industry or a shaft covering repair.

5.2.1 North River Bridge, North Carolina [66]

The systems installed on the North River Bridge pilings in Wilmington, N.C. are an example of fiberglass application to inhibit corrosion, restore strength, and improve appearance of structures. The applied FRP was a pre-impregnated epoxy, capable of water-activation and curing at ambient temperatures, in this case 10° C. Application of the fiberglass cloth was completed after a layer of adhesive was applied, an added step that may not be required on round piles or a shaft. Procedurally, the columns were wrapped, beginning with one complete turn, and then progressively spiraled down the column. Each wrap touched the last, but did not overlap. Once the end of the column was reached, one 360° turn was completed and the spiral continued back up the column. Three FRP layers were installed on the North River Bridge pilings.

5.2.2 Friendship Trails Bridge, Florida [67]

A former road bridge, the Friendship Trails Bridge in Tampa, Florida, now accommodates only pedestrian traffic and stretches 2.6 miles with 254 piles. This study addressed the issues for repairing the piles within a submerged environment and the materials used to accomplish the task. Four piles were chosen for FRP repair. Pile preparation included removing surface defects, filling voids with epoxy, and grinding corners to a minimum ¾ inch radius, thereby eliminating stress concentrations. Two piles were wrapped with the Aquawrap® repair systems designed for piles and pipes,

having a unique pre-impregnated *glass* or *carbon* fabric weave with water-activated resin. The second two piles were wrapped with Tyfo® uni-directional glass fabric weaves impregnated on-site with an underwater epoxy. The piles were wrapped both vertically and transversely, or spirally without overlap, to enhance the FRP properties and restore the strength to the piles.

Particular concern should be given to the adhesive bond in this situation or in others requiring underwater, wet application of FRP and epoxies. This study tested the adhesive performance two years post-installation and found that the Aquawrap® pre-impregnated system performed less favorably in the wet region than the Tyfo®.

Table 9: Test results for Friendship Trails Bridge pile repairs [67].

Pile #	Material / Manufacturer	Top-dry psi (failure)	Bottom-wet psi (failure)
100-N	Carbon Aquawrap®	145.0 (layer)	58.0 (layer)
		116.0 (layer)	0.0 (layer)
		130.5	29.0
100-S	Glass Aquawrap®	0.0 (layer)	0.0 (layer)
		0.0 (layer)	0.0 (layer)
		0.0	0.0
101-N	Glass Tyfo®	101.5 (epoxy)	58.0 (epoxy)
		29.0 (epoxy)	260.9 (concrete)
		65.2	159.0

Table 9 illustrates the study's findings and shows the point of failure during a pull test, given in psi, and the failure location of each specimen. The *carbon* fiber Aquawrap® system was more likely to have interlaminar failure in both the dry and wet regions, while the *glass* fiber Aquawrap® system failed between layers without registering a load. The Tyfo® *glass* fiber system failed in the adhesive bond between the concrete and FRP, and failed at a much higher load in the wet region than the *carbon* fiber Aquawrap® system.

If the bond between the surfaces is corrosion resistant and provides continuous contact, underwater application of FRP to a U.S. Navy shafting is feasible.

5.2.3 Underwater Pipe Wrapping / Curing [68]

While concrete bridge pile examples provide evidence of underwater epoxy and fiber reinforcement, there are issues due to more severe environments that must be addressed for the repair of steel pipes and shafting. The bridge piles repaired experienced an air-water interface subjected to tidal currents and wave action. Table 10 provides a list of materials used during the Friendship Trails Bridge pile repair and subsequent laboratory experimentation. The Tyfo® system was used in both examples because of the specific resin developed for underwater curing and its' adaptability to *carbon* and *glass* fiber applications.

Table 10: Underwater FRP wrap manufacturers and materials [67, 68].

Friendship Trails Bridge Pile Repair	Laboratory Pipe Wrap Experimentation
Manufacturer, Fiber, Resin	
Air Logistics Co.: Aquawrap® System Pre-preg uni- & bi-directional *glass* urethane resin	
Fyfe Co.: Tyfo® system SCH-51A uni-directional *glass* SW-1 epoxy resin	Fyfe Co.: Tyfo® system SCH-41 & 41S uni-directional *carbon* SW-1 epoxy resin
	Silka Canada: Silka-wrap® Hex 230C uni-directional *carbon* Silkadur® Hex 306 epoxy

Six specimens and one control pipe were tested for bending strength. In each case, the specimens underwent surface preparation by grinding with a mechanical brush to remove minor rust formations. Of the six specimens, two were prepared and wrapped

in-air (#2 and 3); two were prepared underwater, wrapped, submerged for 10 weeks, and tested after drying (#4 and 5); and the final two specimens were prepared exactly as specimens 4 and 5, left submerged for 8 weeks, and tested after removal from the saltwater (#6 and 7).

When subjected to four-point bending, these experiments showed that underwater bonding and curing systems provided favorable results and enhanced flexural stiffness and ultimate strength of steel pipes. Seica et. al. [68], suggest that specimen 7 may be better suited for seawater application due to its' superior performance as noted in Table 11. (This hybrid combination was used because the Silka® resin did not appear to cure completely underwater and the Tyfo® fibers were heavy and did not remain in place under their own weight.)

Table 11: Results from application of CFRP to tubular steel structures [68].

	Specimen	Material	Elastic Flexural Stiffness (x10^12 N / mm^2)	Ultimate Strength [kN (%)]
	1	Reference Specimen	1.56	240
Cured "in-air"	2	Silka-wrap®, Hex 230C, Hex 306 epoxy	1.68	279 (+16.0)
	3	Tyfo®, SCH-41, SW-1 epoxy	1.84	305 (+26.9)
Cured Underwater	4	Silka-wrap®, Hex 230C, Hex 306 epoxy	1.61	260 (+8.0)
	5	Tyfo®, SCH-41, SW-1 epoxy	1.73	278 (+16.0)
Cured Underwater	6	Silka-wrap®, Hex 230C, Hex 306 epoxy	1.60	266 (+11.0)
	7	Silka-wrap®, Hex 230C, Tyfo® SW-1 epoxy	1.67	290 (+20.6)

5.3 U.S. Navy Propulsion Shaft Covering Repair

The U.S. Navy's underwater shaft covering procedure was developed to repair the propulsion shaft covering on surface combatants [5, 72]. The primary purpose of the shaft covering is to reduce or eliminate corrosive effects on the shaft. The procedure is normally accomplished in drydock. An underwater procedure was developed to repair a damaged shaft covering in a minimal amount of time without the expense or inconvenience of drydocking. Typical shaft arrangements for U.S. Navy ships are shown in Figure 38.
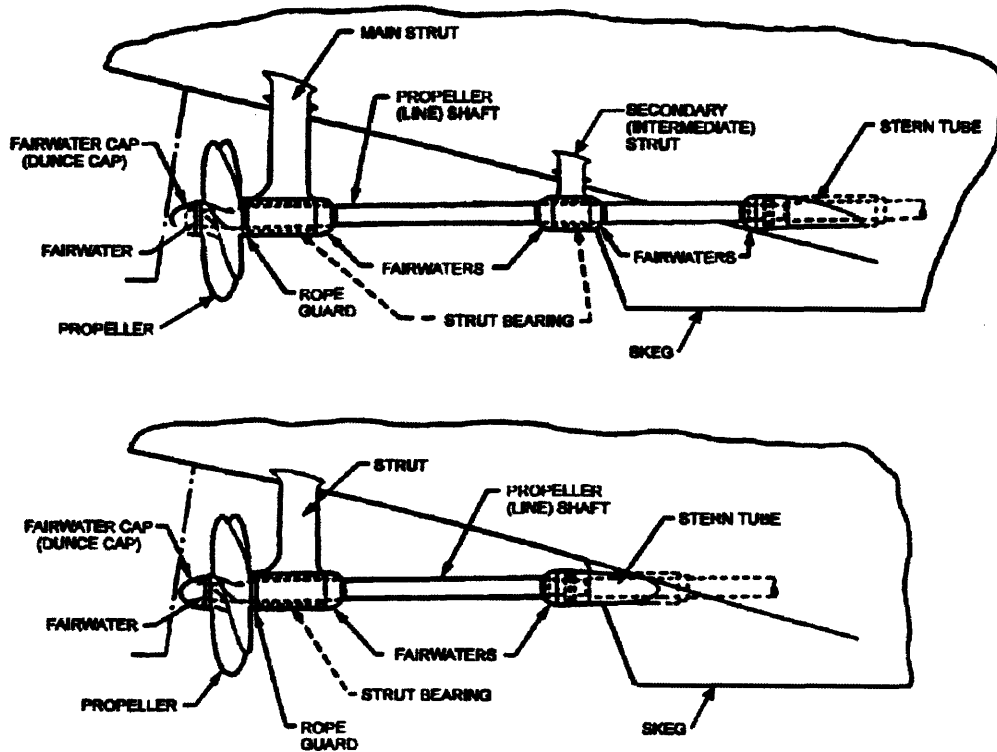
Figure 38: Typical shafting arrangements for U.S. Navy ships [5].

After removal of the existing shaft covering, the traditional procedure involves installing a habitat for the divers to perform work in a dry environment, similar to an underwater bubble after water has been evacuated. This habitat provides a platform for

the divers to stand on while preparing the shaft and applying the repair materials. Primarily, the habitat provides the means to heat the shaft to reduce the cure time of currently approved materials.
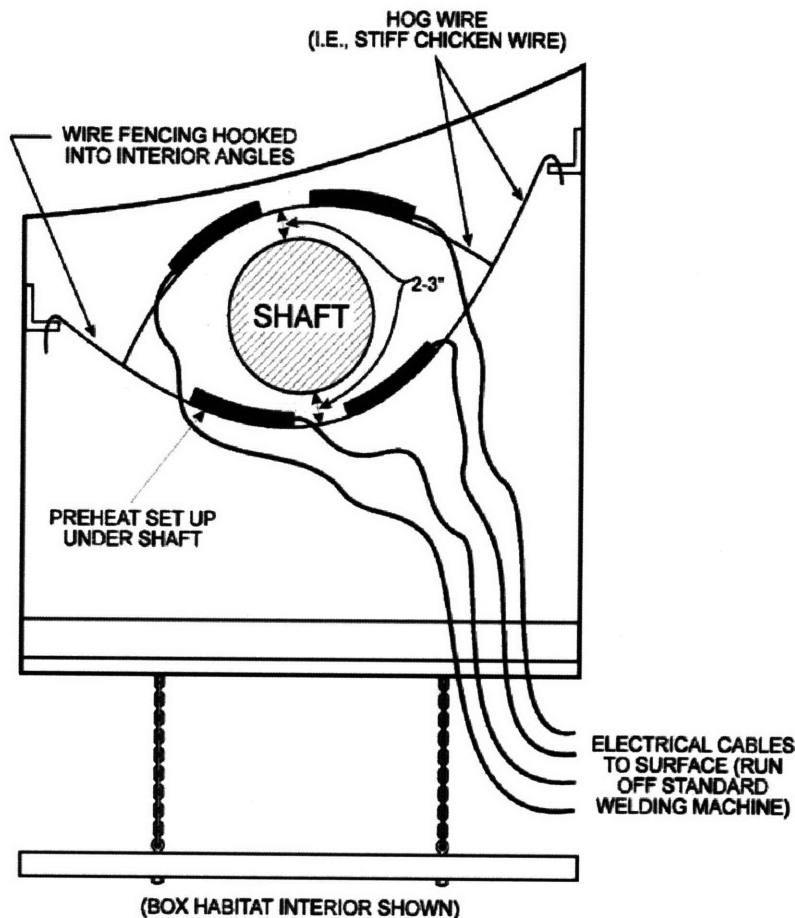
Figure 39: Underwater habitat configuration [5].

The U.S. Navy procedure for shaft coverings requires 4 layers of alternately wrapped FRP cloth in a manner shown in Figure 40. Wrapping begins with a 360° vertical wrap, followed by gradually angled wraps to travel the length of the shaft. Resin is applied before each new layer and after complete saturation of the previous layer in order to prevent air pockets within the laminate. This procedure differs from the procedure described in Section 5.2.3, with the use of four layers versus three. The experimental specimens in Section 5.2.3 were designed for increased strength and

because of that, used two longitudinal layers for stiffness enhancement. The shaft covering, however, is not primarily designed for strength, rather corrosion protection.

CHANGING OF HELIX ANGLE IN
ORDER TO END UP NORMAL (90°)
TO SHAFT AND SLEEVE ℄
(AVOID WRINKLES,
SLASH TAPE IF NECESSARY)

SHAFT AND SLEEVE

BUTT TAPE EDGES AS
CLOSELY AS POSSIBLE

CROSSOVER OF FIRST
AND SECOND PLY

FIRST PLY OF
FIBERGLASS
TAPE

SECOND PLY OF
FIBERGLASS TAPE
BEING APPLIED
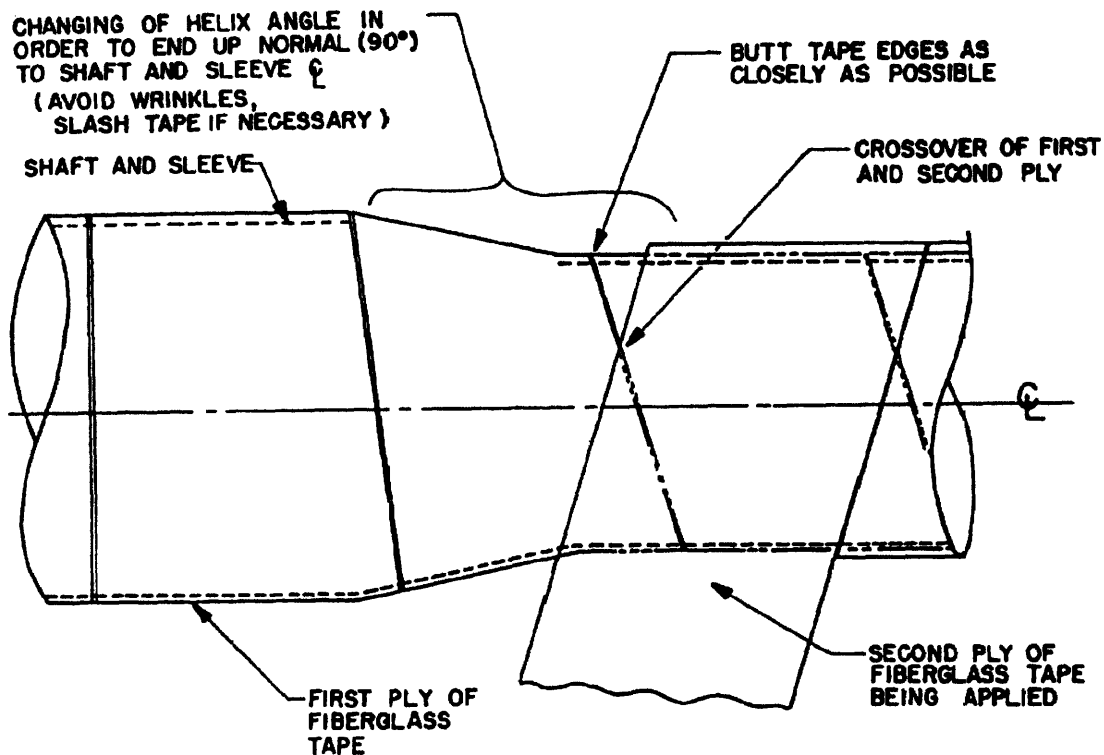
Figure 40: Schematic of FRP wrap [72].

The previous sections prove the feasibility of an underwater system for replacing the shaft covering similar to that used on steel pipe repairs [68]. In addition to simplifying the current procedure, eliminating the cofferdam would also reduce the associated material transportation costs and increase safety for the divers. Working inside a cofferdam poses several risks to the diver including injury caused by rapid flooding should the seal rupture between the hull and the cofferdam. With currently approved dry-cure materials, a loss of seal between the hull of the ship and the cofferdam will cause the replacement shaft covering to be contaminated by saltwater and rendered useless with the associated rapid cooling of the materials.

5.3.1 In-the-wet Repair Factors

The underwater curing systems addressed in Section 5.2.3 provide substantial evidence that replacing a shaft covering can be accomplished in-the-wet with the appropriate precautions. Underwater application of such a system to the shafting of U.S. Navy ships presents several problems, including surface preparation, electrolytic corrosion, possibility of trapping moisture under the wrap, and curing times [5, 72].

Surface Preparation

Removal of existing covering and surface preparation should be in accordance with current standards, including reducing surface imperfections to less than a 3 mm profile and removal of marine fouling, rust, and oxidation deposits [5]. Removal of marine fouling, rust, and oxidation may be accomplished with the use of a wire brush.

Surface preparation in-the-wet may present certain challenges because of the limited availability of bond enhancing chemical treatments such as silane while the work environment is exposed to surrounding saltwater. While this may not be ideal, materials exist and have been tested that provide adequate protection and bonding without chemical surface treatments, Section 5.2.3.

Electrolytic Corrosion

Application of **carbon** mat requires an insulating layer of **glass** mat to prevent electrolytic corrosion. This phenomenon is caused when two carbon compounds adjacent to each other are subjected to a saltwater environment. Saltwater then induces the transfer of electrons between one material acting as the cathode and the other acting as an anode causing the deterioration of the weaker material. As mentioned in Section 4.3.1,

placing a single layer of *glass* mat between a metal material and *carbon* mat will prevent electrolytic corrosion. Thus two solutions exist:

1) In order to provide a simple solution, Tyfo® has manufactured a *carbon* fiber mat with a single layer of *glass* fiber mat affixed to the bottom surface. The material was specifically manufactured for repairs to oil and gas pipelines.

2) The current procedure requires *glass* fiber mat in order to eliminate the hazards associated with electrolytic corrosion between *carbon* mat and steel.

Vacuum / Pressure Application for enhanced bond strength

Increased effectiveness may be demonstrated with the use of a pressure / vacuum system such as that developed by Sen and Mullins [44, 64]. Vacuum bagging, however, may not be suitable in the underwater environment particularly because a seal rupture between the shaft and vacuum bag would introduce saltwater into the curing lamina. Thus, a pressure bagging system that is capable of applying constant pressure to the curing lamina is recommended. In the absence of pressure application, previous experiments have used nylon ties to secure composite pipe wraps during underwater cure with satisfactory results [68].

Cure Time

Cure time is traditionally an issue with resins. The currently approved dry-cure resin requires a dry environment and a minimum shaft surface temperature of $60°$, though $73°$ is recommended. One example of underwater curing polymeric resin provides a functional cure, 20-30%, in 1 to 3 hours and 90-95% cure in 8 to 24 hours [71]. As adhesive technology continues to advance, both *glass* and *carbon* fiber reinforced composite cure time may decrease.

5.4 DDG-1000 Composite Twisted Rudder (CTR)

The DDG-1000 is the most recent acquisition in the U.S. Navy's arsenal with a build contract awarded in February 2008. Though there are many technical advances in the design of this ship, the composite twisted rudder (CTR) is of particular interest. The CTR combines the strength of composite laminates and a foam core with hydrodynamics for decreased drag and reduced weight. Using a 25-layer, **E-glass** composite laminate over a steel frame and foam core, the rudder must transmit directional inputs from the ship to the water and endure very high torsional loads from the hydrodynamic forces from the ship's motion and propeller wash [73]. Figure 41 provides an internal structural depiction of the CTR including the steel hub casting and support structure.
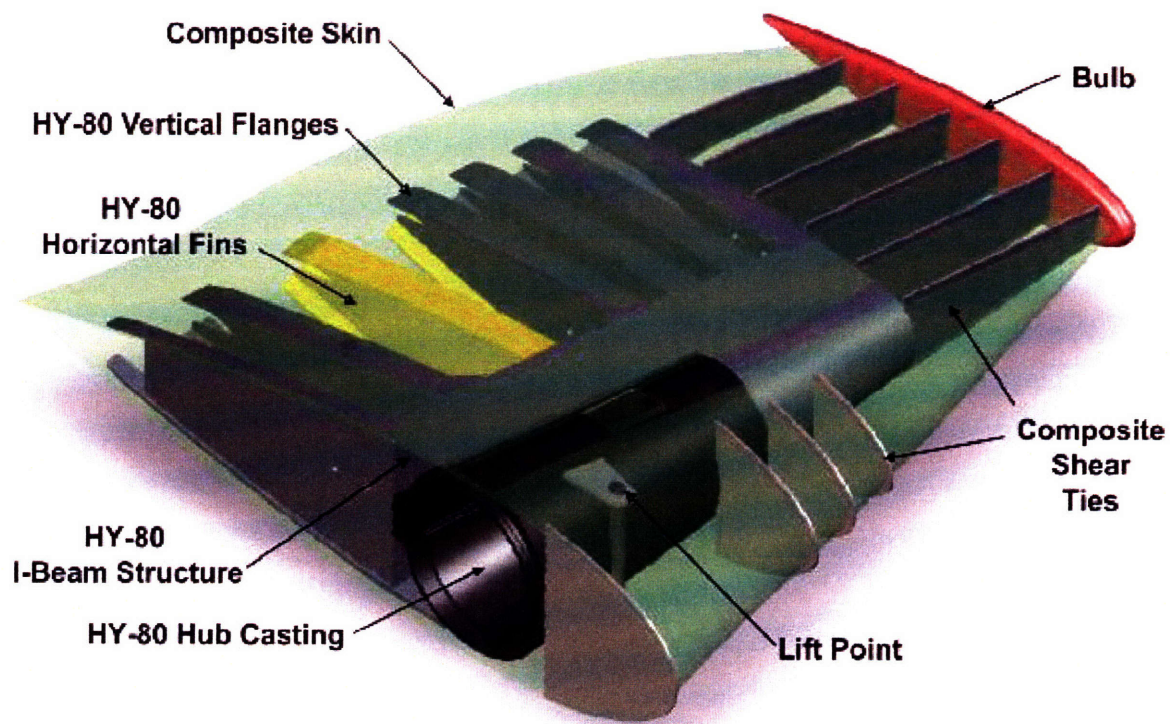
Figure 41: Composite Twisted Rudder Schematic [73].

5.4.1 Underwater CTR Assessment and Repair Theory

Though this design may not enter widespread service for several years, the future may require underwater NDE and repair of the laminate structure. Aside from the underwater environmental complications with NDE and repair, it is perceived that only single-side damage will be considered for underwater repairs. Single-side refers to the accessibility of the structure in which only one side will be available to the operator. If damage encompasses two sides or affects an exceedingly large area, it is assumed that the rudder has suffered extensive damage and will be scrapped and replaced; an operation that may be accomplished underwater.

Chapter 2 addresses NDE methods and potential for underwater assessments. After a thorough visual inspection, ultrasonic and x-ray evaluation have the greatest potential for accurate results.

As the U.S. Navy experienced with the U.S.S. Boone and the FFG-7 class of ships, access to the rudderstock, nut, and retaining pin inside the casting could present significant issues and opportunity for repairs [8]. The FFG-7 class rudder nut modification required removing an access panel on the side of the rudder via carbon arc gouging. Once the access panel was removed, a cofferdam was placed on the side of the rudder to facilitate the repairs and, most importantly, to create a water-free environment to prevent water entrapment inside the steel rudder casing. In the case of a composite rudder, should such access be required, cutting may be performed in a much simpler manner and the use of a dry habitat may ensure proper adhesion to the parent structure.

5.4.2 Single sided repair

Single-side repairs require significant consideration relative to adhesive bonding, structural assessment, and materials associated with either a dry or wet repair environment [25, 37, 44]. These topics have been covered previously in general terms; however, Structural Composites, Inc. provides guidelines for repairs particular to the CTR [73]. The most salient points to consider in the lay-up process are described below.

Taper Angle / Slope

The recommended taper angle, or slope as shown in Figure 42, for the CTR is 12:1 [73]. This is the typical selection for a thick section laminate; however, greater angles can be used if adequate distance between the repair area and edge of the structure remains.

Boundary of removed damage
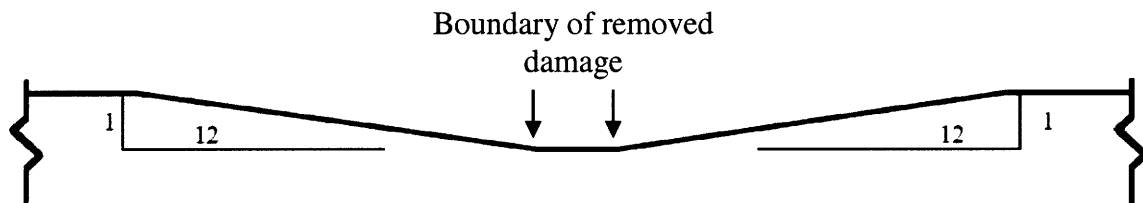
Figure 42: Taper slope [73].

Using the recommended laminate peeler, which is capable of removing ¼ inch each pass and leaving a tapered surface, accomplishes removal of damaged CTR laminate. If specialized tooling is not available underwater, the secondary method of choice is cutting each layer with a grinding disk and peeling the laminate with a chisel. Smoothing of the surface should be accomplished by sanding followed by careful dust removal and surface treatment such as silane for increased bonding effectiveness.

Material selection: Pre-cured versus Co-Cured Patch

Two laminate methods can be used for patch repair: pre-cured or co-cured. Pre-cured patch material selection may increase the quality of the patch and reduce the risk of delaminations between multiple layers if moisture contamination becomes a factor [44]. However, pre-cured requires extensive effort to match the repair patch with the parent repair site. Any large deviations may result in bondline inconsistencies that will result in stress concentrations or inadequate adhesion. The increased time to design, produce, and fit a pre-cured patch could eliminate this option from use on a time-critical job.

The alternative to the pre-cured patch method is called co-cure [44, 73]. Co-cured means each laminate layer is placed individually and cured as it bonds to the repair vice pre-cured which is cured at a manufacturing facility and attached to the repair site with a compatible adhesive. Co-cured patches require a higher level of proficiency by the repair personnel during site preparation and lay-up, but have the advantage of producing a form-fitting patch with relatively little concern about bondline thickness.

For a co-cured patch the primary application parameters are as follows:

- Chopped strand mat (CSM) should be used for the first layer to improve interlaminar bond with the parent laminate.

- Apply resin first to the parent material and work FRP mat into resin to prevent trapped bubbles or dry mat voids. Subsequent FRP layers should be preceded by resin application as well.

- Maintain mat ply direction according to the manufacturer's specifications.

- Apply no more than ¼ inch laminate at a time. More than ¼ inch will induce a greater exothermic reaction that will cause "cooking" of the laminate or patch shrinkage during cooling which will reduce the bonding strength and increase potential for fatigue cracking.

Co-Cure: Pre-preg versus Wet-layup

Two types of co-cured patches can be used: pre-preg or wet-layup. Experimental results shown in sections 5.2.2 and 5.2.3 provide evidence that pre-preg FRP mat does not have reliable adhesive bonding strength for consideration on permanent repairs. Temporary repairs, however, may require fast and adequate patches that can be applied by divers in-the-wet without the use of dry habitats; in which case, pre-preg is an option.

The wet-layup methods described above and experimentally applied in sections 5.2.2 and 5.2.3 do produce reliable bonds between parent material and FRP and could be applied to permanent repairs.

Application Method

Laminate can be laid in two methods, shortest first (Figure 43) or longest first (Figure 44). Shortest ply first, Figure 43, provides a better surface for reinforcing plys on top of the repair as well as eliminating finishing work. Longest first, shown in Figure 44, requires more finishing work to smooth the patch.
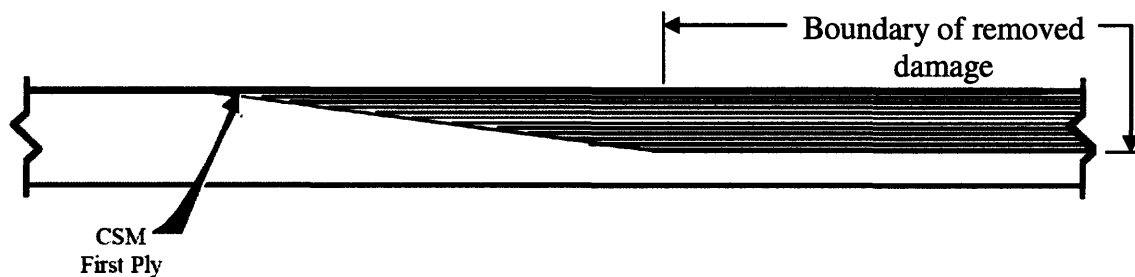
Figure 43: Shortest ply first method [73].
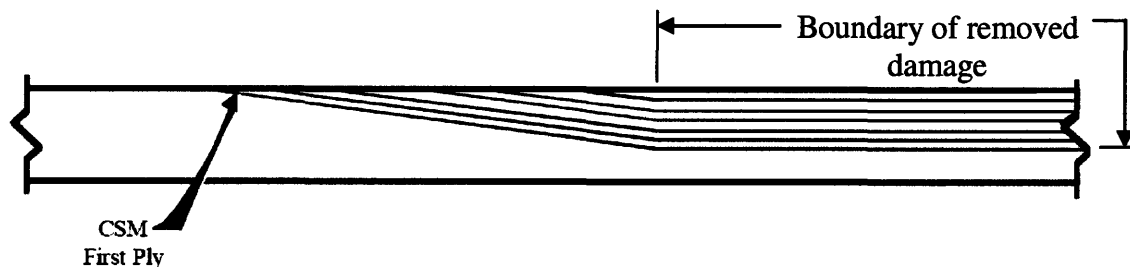
Figure 44: Longest ply first method [73].

5.4.3 Post Repair Assessment [73]

Similar to pre-repair evaluation, the repair should be inspected post-repair for adequacy prior to applying the surface protection. Structural Composites, Inc. requires visual inspection for the following:

- No open voids, cracks, pits, and crazing;

- No evidence of resin discoloration;

- No evidence of dry reinforcement shown by white laminate;

- No wrinkles in the reinforcement and no voids greater than ½ inch diameter.

Additionally, the repair surface should be free of defects and provide a smooth surface for the surface protectant layer. Barcol Hardness tests, if provided by the laminate manufacturer, should be within 10% of the manufacturer's specifications.

If resin voids greater than ½ inch are found, simple repairs may be made by drilling two small holes (3/16 inch); one for resin injection, the other for air release. Once resin has successfully filled the void and cured, the surface should be smooth and free of defects as mentioned above.

If a dry habitat is used in the underwater environment and remains in place, it is recommended to use proven NDE methods for proper inspection of repairs. Additional methods available in a dry environment unhampered by water's absorption properties are thermography or dye penetrant [44].

6

FUTURE RESEARCH & CONCLUSIONS

6.1 Future Research

Throughout this thesis, several shortfalls have been realized due to the underwater physical limitations of current technology and proper damage assessment associated with nondestructive evaluation. First, underwater nondestructive evaluation has not been thoroughly tested on composite material applications. Most nondestructive methods described in Chapter 2 are severely limited by the underwater environment either through temperature diffusion or acoustic wave propagation.

Second, the use of in-situ structural health monitoring (SHM) technology has not been thoroughly explored for uses in the marine environment. At this time, literature reveals only two examples of marine SHM application. The first example can be found on a tanker ship used to provide real-time monitoring of the ship's behavior and diagnose critical points on the hull structure [74]. The second example references a Swedish patrol boat, *HNoMS Skjold* [75]. Extensive testing and use of SHM could greatly enhance the capabilities of future composite structures and reduce over design and maintenance cost. Additionally, underwater components such as the DDG-1000 composite twisted rudder will eventually require inspection; SHM would eliminate the need for divers to conduct NDE, which may produce inferior results compared to SHM data.

Third, the focus of this thesis has been to find a permanent repair method for laminate structures used in the marine environment and to hypothesize about their repair with laminates. If for no other reason than to expand the options of materials available to

the salvage engineer, further research should be conducted into the use of materials such as two-part epoxies. Several manufacturers provide two-part epoxies that have been applied by divers for underwater patching and steel repair with documented results; the U.S.S. San Francisco and M/V Tong Chen are two examples [6, 77]. Miko Plaster® is a heavy duty magnetic tarpaulin material that combines a magnetic rubber compound with reinforced fiber technology to provide strength against damage as a result of collisions or groundings and was developed specifically for ship salvage operations. [76].

6.1.1 Underwater NDE Validation Experiment

Given the age of previous experimental data and the underwater NDE methods tested, a validation experiment should be conducted with composite applications similar to the DDG-1000 composite twisted rudder (CTR) using current nondestructive evaluation equipment. The DDG-1000 rudder is built with a 25-layer *E-glass / Vinyl Ester* laminate shell over a steel frame and foam core. In order to accurately test NDE equipment and observations, roughly 20 identical *E-glass / Vinyl Ester* laminate panels should be constructed with the same Vacuum Assisted Resin Transfer Molding (VARTM) process as the CTR to ensure similar fiber volume content. Of those panels approximately 75% should be damaged by impact or differing degrees of flexural strain to simulate hydrodynamic forces and damage. Voids may be simulated with paper or foil embedded in the resin between laminate layers. Erosion and Corrosion damage should not be a factor with the CTR and may be eliminated from simulation due to the protective epoxy layer applied to the rudder skin, which provides visual cues to deterioration.

Commercially available equipment for underwater nondestructive evaluation must meet the minimum standard requirements for operational safety and guidelines set forth by the Supervisor of Salvage and Diving and the published approved equipment list. If

possible, the evaluation process should examine a minimum of three different manufacturer's equipment for each of the methods tested in order to remove individual diver's capabilities from the evaluation process. In each case, the equipment manufacturer should be on hand to provide technical assistance and ensure proper operation of the equipment.

The experiment should gather the following measurements:

- Defect detection versus a known defect.
- Defect detection versus no known defect.
- Location and length of defects.
- Rate of evaluation.

A thorough evaluation and recording of these parameters for each piece of equipment and all specimens should provide the necessary data for determining the accuracy of the NDE method, not the diver or the equipment. The defect detection versus a known defect and detection where no defect occurs will produce a percent success and percent error, respectively. Location and length of observed defects measured against the known x-ray lengths should provide a snapshot of accuracy. The rate of evaluation plotted against accuracy of detection should provide a learning curve for the divers and aid in eliminating data that do not correlate.

Experimental controls should be applied to ensure accuracy. The specimens must be subjected to x-ray inspection prior to the experiments and after completion of all testing. Comparison of the specimen x-rays should provide the basis for calculating percentage accuracy for length and location of defects. Careful handling of the specimens should ensure no damage occurs during the experiment. The most accurate test results may be found using a grease pencil for marking on the specimens, however,

the markings should be removed to eliminate false negative or positive errors that could be generated during a second round of tests.

6.1.2 In-Situ Structural Health Monitoring

In-situ structural health monitoring (SHM) encompasses the use of acoustic or optic sensors permanently embedded, installed on, or placed in the vicinity of composite structures [14]. Acoustic, Extrinsic Fabry-Perot Inferometry (EFPI), and Fiber Bragg Grating (FBG) sensors are the most common types of SHM devices used today; FBG sensors are the most widely used due to their simplicity and ease of multiplexing [78]. In any case, data collected from smart structures may include stress, strain, fatigue, damage analysis, and moisture ingression.

Acoustic emission monitoring sensors have been used for several years in seismology for triangulating the source of earthquakes [63]. This method of assessment uses the wave propagation velocity to determine the location of the epicenter as measured from acoustic sensors on the surface of the structure. Acoustic sensing's primary disadvantage is an inability to provide useful and accurate results in a low signal-to-noise ratio environment. Such an environment would be especially prevalent in operational naval structures that endure constant motion and stress induced vibrations [16, 63].

Fiber optic sensors (FOS), both EFPI and FBG, read changes in the phase of light waves that travel through the fiber optic sensor [18]. Because temperature and strain states of the surrounding material directly affect the reflectivity spectrum of the light passing through the FOS, these sensors can provide insight to the real-time state of the parent structure [80]. Comparison between FOS and conventional strain gages has shown correlation with less than a 5% measurement difference with the added benefit of

FOS being lighter, smaller, having immunity to electromagnetic interference, and a capacity for multiplexing [18].

Fabry-Perot sensors, Figure 45, are termed "extrinsic" because of the cavity between the fiber ends, resulting in a sensor output that is immune to perturbations in the input and output fibers caused by transverse loading [18, 82]. Inside the capillary housing, one fiber end acts as a lead-in/lead-out source, where as the other is a mirror reflecting the light signal back [16]. EFPI sensors, because of the rigid micro-capillary housing, limit the data to longitudinal directions and increase the resin void around the sensor resulting in stress concentrations; a factor compounded by orthogonal sensor orientations [18].
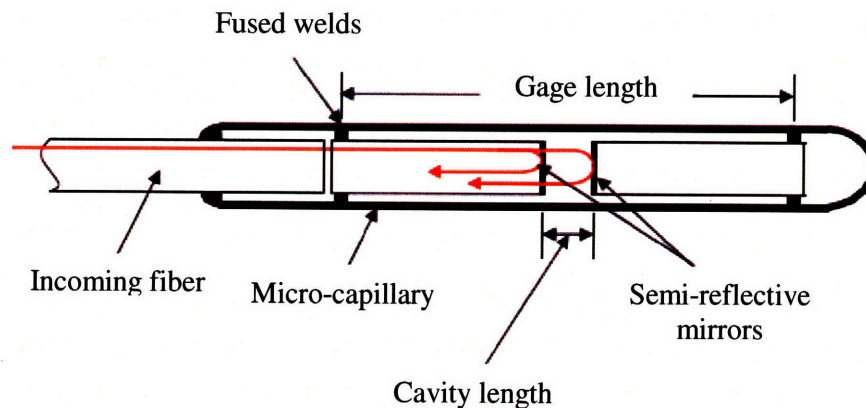
Figure 45: Extrinsic Fabry-Perot Interferometric fiber optic sensor [20].

Fiber Bragg Grating sensors, Figure 46, although more simple, are based on similar technology without the capillary housing and air-gap and are generally much smaller diameter fibers than the EFPI. FBG sensors operate on the concept of selectively reflecting a single wavelength while continually transmitting another [79, 81]. In doing this, FBG sensors are particularly adaptive to multiplexing with many sensors on one fiber spaced at known intervals and protected by the cladding and jacket. The simplicity

of construction compared to that of the EFPI makes FBG sensors particularly adaptable to use in composite laminate structures and results in a higher failure strain of 2% versus 1.2% for EFPI sensors [16].
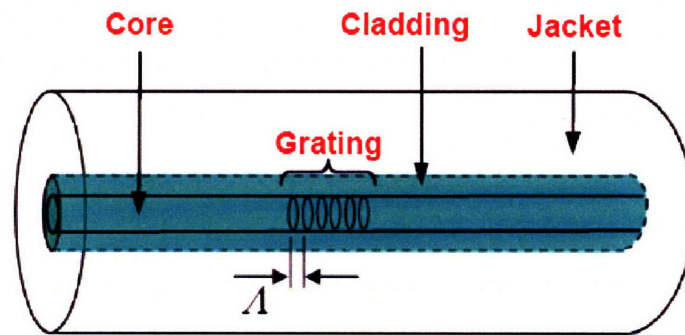
Figure 46: Fiber Bragg Grating (FBG) sensor [81].

Advantages of SHM

SHM provides several distinct advantages during manufacture, construction, and life-cycle analysis. Although not immediately beneficial, structures employing SHM sensors will provide insight into the overdesign of certain structures. History has shown multiple examples of structures with inordinately high safety factors, routinely 4-6 times, due to a lack of understanding of loading or environment [50]. Through analysis of data provided by sensing structures, future designs may result in reduced structural weight by reducing overdesign and could be built to withstand accurate loading profiles.

SHM instrumentation will decrease maintenance cost due to the shift from planned maintenance to required maintenance. In the case of naval vessels, a design with decreased structural weight will result in decreased fuel usage [17]. Additionally, sensing structures will provide constant self interrogation to determine temperature, vibration, structural integrity, damage state, and deformation stress [79].

Sensor Embedding Issues

Sensor embedding within composite laminate structures presents concern due to increasing resin pockets, which create stress concentrations around the sensors and may lead to potential debonding between layers [79]. Specifically, optical fiber diameter, orientation, placement, and coating have been cited as the most relevant factors for embedment of sensors.

Optical fibers embedded between layers of composite lamina create void spaces reducing the structural integrity of the material. In order to minimize this effect, optical fibers with a diameter of less than 140 μm should be employed as they do not appear to reduce ultimate tensile strength or the fatigue life of *graphite / epoxy* specimens [79].

Ingress and egress locations of the sensor lead in the laminate cause inconsistencies in the laminate surface, which further reduce the strength of the material as well as causing the sensor lead to bend, possibly resulting in sensor failure. Solutions to this problem include Teflon sheathing or super gluing the leads to the surface to prevent breakage [18].

The most common result of embedding sensors is the reduction in the strength of the parent structure. In order to prevent strength loss, optical strain or temperature sensors should be embedded between laminae with the same fiber orientation [18, 84]. Aligning the sensor in parallel with the surrounding fibers prevents resin rich areas around the sensor and minimizes non-uniform stress fields, which will limit the accuracy. However, if the sensor provides damage detection information, optimum results occur when the sensor is embedded as close to the surface of maximum tensile strain as possible and oriented orthogonally between collinear layers [18, 85]. Data suggest that compressive strength for orthogonally embedded sensors may be reduced by as much as 26% [84]. In the case of a much larger embedded Fabry-Perot fiber optic rosette sensor

in neat resins and polymer matrix composites, Figure 47, the compressive strength was reduced by two-thirds [18, 19].
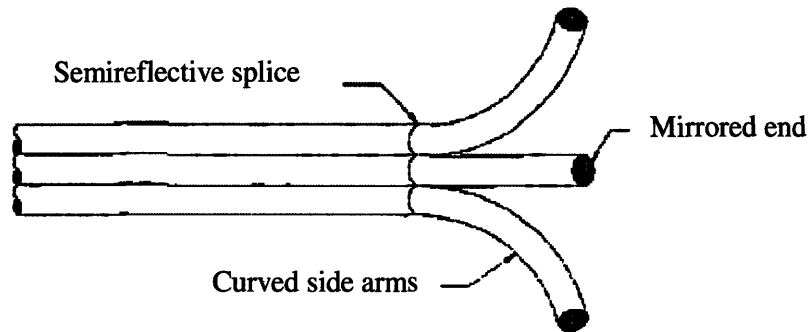
Figure 47: Fabry-Perot rosette sensor [19].

Data below provide information concerning the mechanical effects of embedded EFPI sensors in *E-glass / vinyl ester* composite laminates [18]. As previously discussed in Section 4.3.1, this combination was chosen for impact resistance, low cost, and good performance in marine environments. These experiments used a 350 μm diameter EFPI fiber optic sensor embedded in both parallel and perpendicular orientations. The notation T0 signifies a parallel sensor / fiber orientation, while T90 indicates a perpendicular arrangement. Table 12 and Table 13 show direct comparisons of experimental results. While compressive strength showed little effect, longitudinal tensile strength was reduced by 20-30% and transverse tensile strength was reduced by 5-10%.

Table 12: Effect of embedded sensors on tensile properties [18].

Mechanical Property	With Embedded Sensors				Control (No Embedded Sensors)			
	Mean (MPA)	COV (%)	Mean (MPA)	COV (%)	Mean (MPA)	COV (%)	Mean (MPA)	COV (%)
	Panel TO-1		Panel TO-2		Panel TO-1		Panel TO-2	
Fiber Volume Ratio, (%)	54.8		51.7		54.8		51.7	
Longitudinal Modulus	39,670	3.3	46,347	35.5	39,538	1.8	39,338	4.1
Longitudinal Tensile Strength	662.1	31.4	486.8	27.6	842.1	3.3	720.6	4.7
	Panel T90-1		Panel T90-2		Panel T90-1		Panel T90-2	
Fiber Volume Ratio	54.3		54.6		54.3		54.6	
Transverse Modulus	11,960	10.7	12,030	14.2	12,040	9	11,530	3.8
Transverse Tensile Strength	29.1	16.2	29.32	16.4	31.95	11.5	32.27	4.7

Table 13: Effect of embedded sensors on compressive mechanical properties [18].

Mechanical Property	With Embedded Sensors				Control (No Embedded Sensors)			
	Mean (MPA)	COV (%)	Mean (MPA)	COV (%)	Mean (MPA)	COV (%)	Mean (MPA)	COV (%)
	Panel CO-1				Panel CO-1			
Fiber Volume Ratio, (%)	53.0				53.0			
Longitudinal Modulus	36,190	34.6			39,597	13.1		
Longitudinal Compressive Strength	426.5	5.7			385.2	25.9		
	Panel C90-1		Panel C90-2		Panel C90-1		Panel C90-2	
Fiber Volume Ratio	41.4		53.6		41.4		53.6	
Transverse Modulus	9,184	19	11,365	7.9	8,438	11.7	10,249	23.5
Travsverse Compressive Strength	92.35	5.5	100.6	2.8	94.58	4.8	102.8	4.2

In some cases, EFPI sensors have even less effect on material properties in static loading and fatigue testing than the above data suggests [83].

Considerations

Further consideration of fiber optic sensor technology should be a high priority in industries dependent on accurate engineering, structural design, and weight reduction. Current overdesign of civil, naval, and industrial systems results in added manufacturing and maintenance costs.

6.2 Conclusions

The result of this work is an understanding of requirements needed for the successful underwater assessment and repair of composite structures. Both nondestructive evaluations and repair of composites at or below the waterline present a number of unique challenges due to the environment. In the near future, underwater NDE could be aided by the use of ultrasonic C-scan technology or the use of in-situ structural health monitoring; either case would enhance working knowledge and structural assessment of composites in order to conduct successful permanent repairs.

Repairs of composites below the waterline have been examined and proposed for application for select U.S. Navy ship components. Throughout this investigation, material selection was found to be a dominant factor for successful repairs. Current procedures emphasize removing damaged composites from moist or wet environments. Further, selecting a material compatible with the parent surface and the surrounding environment are more important than the specifics of the patch design. As technology evolves and provides better underwater curing characteristics of advanced composites, more complex repairs may be achievable underwater.

1   Boeing. < http://www.boeing.com>. January 2008.

2   Dow, R.S., and Bird, J. "The Use of Composites in Marine Environments." Structural Materials in Marine Environments. The Royal Society. London: 1994.

3   Noury, P., Hayman, B., McGeorge, D., and Weitzenbock, J. "Lightweight Construction for Advanced Shipbuilding – Recent Development." Det Norske Veritas, Norway. 2002.

4   Batholomew, C.A., Marsh, B., and Hooper, R.   Salvage Engineering. Washington, D.C.: Naval Sea Systems Command, 1992.

5   Underwater Ship Husbandry Manual. Naval Sea Systems Command. Feb 2007. <http://supsalv.org/manuals/uwsh/intro.html>.

6   Hagan, W.L. "USS Frank Cable Divers Shine in the USS San Francisco Emergency Response." FACEPLATE. Vol. 9. (2005): 22-23.

7   Mine Countermeasures Ships - MCM. <www.Navy.mil>. January 2008.

8   Young, J. A. "Emergent Underwater Rudder Replacement on USS BOONE (FFG-28)." FACEPLATE. Vol. 11. (2007): 3-5.

9   Conversations with LCRD C. Parks. NAVSEA 00C58. January 2008.

10   Greene, E. "Composite Rudders Take Shape for U.S. Navy." Composites Manufacturing. Vol. 22. No. 10. (2006).

11   Sharp, D. "Maine Shipyard seeks to build better patrol boat for special ops." <www.boston.com>. 11 January 2008.

12   UMC International. "A passenger vessel receives red carpet treatment at Tenerife by UMC's specialist combination team of naval architect and hull plating repair divers." <www.umc.co.uk>. Dec. 2003.

13   Camponeschi, E.T., Crane, R., Lipetzky, K., and Bandos, B. "Role and Use of Nondestructive Testing for U.S. Navy Composiet Ship Structures." Materials Evaluation Vol. 65. (2007): 752-758.

14   Pollock, A.A. "Loading and Stress in Acoustic Emission Testing." The American Society for Nondestructive Testing. March 2004.

15   Chang, P.C. and Liu, S.C. "Recent Research in Nondestructive Evaluation of Civil Infrastructures." Journal of Materials in Civil Engineering. (2003): 298-304.

16   Zhou, G., and Sim, L.M. "Damage detection and assessment in fibre-reinforced composite structures with embeded fibre optic sensors-review." Smart Materials and Structures. Vol. 11. (2002): 925-939.

17   Beral, B., and Speckmann, H. "Structural Health Monitoring (SHM) for Aircraft Structures: A Challenge for System Developers and Aircraft Manufacturers." Structural Health Monitoring. Chang, Fu-Kuo ed. 2003.

18   Lopez-Anido, R., and Fifield, S. "Experimental Methodology for Embedding Fiber Optic Strain Sensors in Fiber Reinforced Composites Fabricated by the VARTM/SCRIMP Process." Structural Health Monitoring. Chang, Fu-Kuo ed. 2003.

19   Valis, T., Hogg, D., and Measures, R. M. "Fiber-Optic-Fabry-Perot Strain Rosettes." Smart Materials and Structures. Vol.1 (1992): 227-232.

20   Haskell, A.B. "A Durability and Utility Analysis of EFPI Fiber Optic Strain Sensors Embedded in Composite Material for Structural Health Monitoring." Masters Thesis, University of Maine. 2006

21   Ganas, M.J, "Underwater Inspections: The Right Way and the Wrong Way." Undewater. 2003.

22   Childs, K. M., Underwater investigations : Standard practice manual. Reston, Va.: American Society of Civil Engineers. 2001.

23   Ruben, R.L. Materials in Marine Technology. London: Springer-Verlag, 1994.

24   U.S. Departement of Transporation. Reliability of Visual Inspection for Highway Bridges. Vol. 1: Final Report. 2001.

25   Armstrong, K.B., Bevan, L.G., and Cole, W.F. Care and Repair of Advanced Composites. Pennsylvania: SAE International, 2005.

26   Geier, M.H., Quality Handbook for Composite Material. London: Chapman & Hall, 1994.

27   Ray, B.C. "Evaluation of Defects in FRP Composites by NDT Techniques." Reinforced Plastics and Composites. Vol. 26, No. 12 (2007): 1187-1192.

28   Pollock, A.A. "Loading and Stress in Acoustic Emission Testing." Materials Evaluation. March 2004.

29   Shepard, S.M. "Thermography of Composites." <u>Materials Evaluation</u> Vol. 65. (2007): 690-696.

30   Adams, R.D. <u>Adhesive Bonding</u>. Cambridge: Woodhead Publishing, 2005.

31   Goldberg, L. "The Use of Eddy Current for Ferritic Weld Testing in Nuclear Power Plants." <u>Materials Evaluation</u>. 2003.

32   Goldberg, L. "Eddy Current Testing, an Emerging NDT Method for Ferritic Weld Inspection." <u>Materials Evaluation</u>. February 1998.

33   Achenbach, J.D. "Quantitative nondestructive evaluation." <u>International Journal of Solids and Structures</u>. Vol. 37. (2000): 13-27.

34   Ayorinde, E., Gibson, R., Kulkarni, S., Deng, F., Mahfuz, H., Islam, S., and Jeelani, S. "Reliable low-cost NDE of composite marine sandwich structures." <u>Composites: Part B</u>. Vol. 39. (2008): 226-241.

35   Department of Energy. "The Effectiveness of Underwater Non-Destructive Testing." Offshore Technology Report. OTH 84 203. HMSO. London: 1984.

36   Kutz, M. <u>Handbook of Materials Selection</u>. New York: John Wiley & Sons. 2002.

37   Peters, S.T., et. al. <u>Handbook of Composites</u>. London; New York: Chapman & Hall. 1998.

38   Anderson, M.T., Cumblidge, S.E., and Doctor, S.R. "An Assessment of Remote Visual Testing of System Capabilities for the Detection of Service Induced Cracking." <u>Materials Evaluation</u>. September 2005.

39   U.S. Department of Defense. <u>Composite materials handbook</u>. MIL-HDBK-17-3F. Washington, D.C.: U.S. Dept. of Defense. 2002.

40   Wegman, R. F. and Tullos, T.R. <u>Handbook of adhesive bonded structural repair</u>. Park Ridge, N.J., U.S.A.: Noyes Publications. 1992.

41   Berke, M. "Nondestructive Material Testing with Ultrasonics – Introduction to basic principles." <u>NDT.net</u>. Vol. 5. No. 9. Sept 2000.

42   "Ultrasonic Testing Equipment." U.S. Department of Transportation. Federal Highway Administration. < http://www.tfhrc.gov/infrastructure/nde/>. January 2008.

43   Young, J. A. "USS Boone (FFG-28) Emergent Underwater Rudder Replacement." <u>Naval Engineers Journal</u>. American Society of Naval Engineers. Vol. 119. No. 4. (2007): 31-36.

44   Duong, C.N. and Wang, C.H. Composite Repair. Oxford: Elsevier. 2007.

45   American Bureau of Shipping. "Aluminum and Fiber Reinforced Plastics." Rules for Materials and Welding. New York: ABS. 2005.

46   De La Osa, O., Alvarez, A.N., Martinez Mammone, E., and Vazquez, A. "Loss of Mechanical Properties by Water Absorption of Vinyl-ester Reinforced with Glass Fiber." Journal of Reinforced Plastics and Composites. Vol. 25, No. 2. (2006): 215-221.

47   Gama, B. A., Mahdi, S., Cichanowski, C., Yarlagadda, S. and Gillespie Jr., J. W. "Static and Dynamic Strength of Scarf-Repaired Thick-Section Composite Plates." Joining and Repair of Composite Structures. ASTM STP 1455, K.T. Kedward and H. Kim, Eds,. ASTM International, West Conshohocken, PA, 2004.

48   Charalambides, M. N., Hardouin, R., Kinloch, A. J. and Matthews, F. L. "Adhesively-bonded repairs to fibre-composite materials I: Experimental." Composites Part A. Vol. 29A. (1998): 1371-1381.

49   Wang, C.H., and Gunnion, A. "On the design methodology of scarf repairs to composite laminates." Composites Science and Technology Vol. 68, (2008): 35-46.

50   Zhang, S. and Karbhari, V. M. "Evaluation of Property Retention in E-Glass/Vinylester Composites after Exposure to Salt Solution and Natural Weathering." Journal of Reinforced Plastics and Composites. Vol. 19, No. 9. (2000): 704-731.

51   Fortenbery, N. L. "Analysis and Synthesis of Structured Systematic Design Theories." PhD Thesis. Massachusetts Institute of Technology. May 1991.

52   Reid, S.R. and Zhou, G. Impact Behaviour of fibre-reinforced composite materials and structures. Cambridge, UK: Woodhead Publishing. 2000.

53   Saito, H., and Kimpara, I. "Effect of Water Absorption on Compressive Strength after Impact and Post Impact Fatigue Behavior of Woven and Knitted CFRP Laminates." Advances in Composite Materials and Structures. Switzerland: Trans Tech Publications. 2007.

54   Gasem, Z. M. "Environmental Degredation of Flexural and Fracture Properties of Glass/Vinyl Ester Filament Wound Pipes." Key Engineering Materials. Vols. 334-335. (2007): 501-504.

55   Hodgkiess, T., Cowling, M. J., and Mulheron, M. "Durability of Glass-Rienforced Polymer Composites in Marine Environments." Structural Materials in Marine Environments. London: The Royal Society. 1994.

56   Knox, E. M., Hashim, M. J., Cowling, M. J., and Winkle, I. E. "Performance of Adhesively Bonded Structural Components for Marine Structures." Structural Materials in Marine Environments. London: The Royal Society. 1994.

57   Roach, D., Rachow, K., and Dunn, D. "Installation of Adhesively Bonded Composites to Repair Carbon Steel Structure." Joining and Repair of Composite Structures. ASTM STP 1455, K.T. Kedward and H. Kim, Eds,. ASTM International, West Conshohocken, PA, 2004.

58   Mortensen, F. and Thomsen, O. T. "Analysis of adhesive bonded joints: a unified approach." Composites Science and Technology. Vol. 62. (2002): 1011-1031.

59   Tsai, M. Y. and Morton J. "The effect of a spew fillet on adhesive stress distributions in laminated composite single-lap joints." Composite Structures. Vol. 32. (1995): 123-131.

60   Hu, F. Z. and Soutis, C. "Strength prediction of patch-repaired CFRP laminates loaded in compression." Composites Science and Technology. Vol. 60. (2000): 1103-1114.

61   Mail, S. and Ramamrthy, G. "Effect of bond thickness on fracture and fatigue strength of adhesively bonded composite joints." International Journal of Adhesion and Adhesives. Vol. 9. No. 1. (1989): 33-37.

62   Hexcel Composites. "Composite Repair." April 1999.

63   Paget, C.A., Atherton, K., and O'Brien, E.W. "Triangulation Algorithm for Damage Location in Aeronautical Composite Structures." Structural Health Monitoring. Chang, Fu-Kuo ed. 2003.

64   Sen, R., and Mullins, G. "Bond Enhancement for Underwater Pile Repair." Department of Civil and Environmental Engineering. Division of Patents and Licensing. University of South Florida. 2007.

65   Shivakumar, K.N., Swaminahan, G., Sharpe, M. "Carbon/Vinyl Ester Composites for Enhanced Performance in Marine Applications." Journal of Reinforced Plastics and Composites. Vol. 25. No. 10. (2006): 1101-1116.

66   Bazinet, S., Cercone, L., and Worth, F. "Composite FRP Moves into Underwater Repair Applications." Society for the Advancement of Material and Process Engineering. Vol. 39. No. 3. (2003): 8-16.

67   Sen, R. and Mullins, G. "Application of FRP composites for underwater piles repair." Composites: Part B. 38 (2007): 751-758.

68   Seica, M. and Packer, J. "FRP materials for the rehabilitation of tubular steel structures for underwater applications." Composite Structures. Vol. 80. (2007): 440-450.

69   Seeman Composite Resin Infusion Molding Process. U.S. Navy. <http://p2library.nfesc.navy.mil/P2_Opportunity_Handbook/2_II_4.html>. 1 April 2008.

70   Mullins, G., Sen, R., Kwang, S.S., and Winters, D. "A Demonstration of Underwater FRP Repair." Concrete International. (2006): 70-73.

71   Smith, G., Hassan, T., and Rizkalla, S. "Bond Characteristics and Qualifications of Adhesives for Marine Applications and Steel Pipe Repair." North Carolina State University.

72   Department of Defense. "Glass Reinforced Plastic Covering for Propeller Shafting." Military Standard. NAVSEA. MIL-STD-2199(SH). May 1990.

73   Structural Composites, Inc. <www.ctrudder.com>.

74   RocTest Group. "Tanker Ship Hull Structural Monitoring with Smartec's fiber optic solution." December 2007.

75   Wang, G., Pran, K., Sagvolden, G., Havsgard, G. B., Jensen, A. E., Johnson, G. A., and Vohra, S. T. "Ship hull structure monitoring using fiber optic sensors." Smart Materials and Structures. Vol. 10. (2001): 472-478.

76   Michelsen, Nicolai. "Salvaging Damaged Vessels: Keeping the Water Out and the Oil In." UnderWater Magazine. March/April 2003.

77   Dowling, Keith. "Navy Reparis Chinese Merchant Ship." Navy News. February 2007.

78   Light Structures AS. "Fiber Optic Structural Health Monitoring in Oil Production and Transport." The Oil & Gas Review. Vol. 2. (2003).

79   Measures, R. M. "Fiber Optic Sensor Considerations and Developments for Smart Structures." SPIE. Vol. 1588. Fiber Optic Smart Structures and Skins IV. (1991): 282-299.

80   Wippich, M. and Dessau, K. L. "Tunable Lasers and Fiber-Bragg-Grating Sensors." The Industrial Physicist.

81   Kim, M. H., Son, J. Y., Kang, S. W., Lee, J. M. and Na, S. S. "Structural Health Monitoring for Insulation Panels of LNG Carriers using Fiber Optic Sensors." SPIE. Vol. 6176. (2006).

82   Murphy, K. A., Gunther, M. F., Ashish, M. V., and Claus, R. O. "Fabry-Perot fiber optic sensors in full-scale fatigue testing on an F-15 aircraft." SPIE. Vol. 1588. (1991): 134-142.

83   Lee, D., Mitrovic, M., Stewart, A., Richards, L., and Carman, G. P. "Experimental evaluation of embedded EFPI optical fiber sensors for structural health monitoring." Smart Structures and Materials. Vol. 4327. (2001): 753-762.

84   Roberts, S. S. J. and Davidson, R. "Mechanical Properties of Composite Materials Containing Embedded Fibre Optic Sensors." SPIE. Vol. 1588. (1991).

85   Pearson, J., Prabhugoud, M., Zirky, M., Peters, K., Sitar, M., and Davis, L. "Failure and Dammage Identification in Woven Composites with Fiber Bragg Grating Sensors." North Carolina State University. 2005.

86   Williams, James H., Jr., Lee, S.S. "Promising Quantitative Nondestructive Evaluation Techniques for Composite Materials." Materials Evaluation Vol. 43. (1985): 561-565.

87   Thomas, Anton F.; Cai, Liang-Wu; Williams, James H. "Nondestructive Testing of Polymeric Composite Sandwich Panels Via the Thermographic Halo." Materials Evaluation Vol. 60. (Nov 2002): 1339-1349.

88   Cai, Liang-Wu; Williams, James H. "One Dimesnsional Modeling of Ultrasonic Characterization of Face Sheet Core Debonding in Composite Sandwich Panels." Materials Evaluation Vol. 59. (Nov 2001): 1320-1328.

89   Raine, Alan. "The Development and Role of Nondestructive Testiing in the UK Offshore Industry." Materials Evaluation Vol. 59. (Nov 2001): 1299-1305.

90   Nagem, Raymond; Seng, Jocelyn M.; Williams, James H. "Residual Life Predictions of Composite Aircraft Structures via Nondestructive Testing, Part 1: Prediciton Methodology and Nondestructive Testing." Materials Evaluation Vol. 58. (Sept 2000): 1065-1074.

91   Nagem, Raymond; Seng, Jocelyn M.; Williams, James H. "Residual Life Predictions of Composite Aircraft Structures via Nondestructive Testing, Part 2: Degradation Modeling and Residual Life Prediciton." Materials Evaluation Vol. 58. (Nov 2000): 1310-1319.

92   Cai, Liang-Wu, Thomas, Anton F., Williams, James H. "Thermographic Nondestructive Testing of Polymeric Composite Sandwich Panels." Materials Evaluation Vol. 59 (Sept 2001): 1061-1071.

93   Miller, Paul H. Durability of Marine Composites. Dissertation. University of California, Berkeley. April 2000.

94   Miller, Paul H. "Marine Composites Design, Part 1." Professional Boatbuilder Magazine. February/March 2007.

95   Miller, Paul H. "Marine Composites Design, Part 2." Professional Boatbuilder Magazine. April/May 2007.

96   Jenkins, C.H. Manual on Experimental methods for mechanical testing of composites. 2nd ed. The Fairmont Press, Inc. 1998.

97   Piggot, Michael. Load Bearing Fibre Composites. 2nd ed. Kluwer Academic Publishers. 2002.

98   Pendleton, R., Tuttle, M.E. Manual on Experimental Methods for Mechanical Testing of Composites. Society for Experimental Mechanics. 1989.

99   Greszczuk, L.B. Foreign Object Impact Damace to Composites. American Society for Testing and Materials. 1975.

100   Ashton, J.E., Whitney, J.M. Theory of Laminated Plates, Progress in Materials Science Series. Vol IV. Technomic Publishing Co., Inc. 1970.

101   Panagiotidis, Dimitrios. "Adhesively Bonded Composite Repairs in Marine Applications and Utility Model for Selection of Their Nondestructive Evaluation." Master's Thesis. Massachusetts Institute of Technology. 2007.

102   Jones, Daron, "Thin Film Technology's Hull Repair System." UnderWater Magazine. July/August 2004.

103   Jones, Daron. "Case Studies: Search & Salvage." UnderWater Magazine. November/December 2001.

104   Fletcher, Barbara. "The U.S. Navy's Master Plan: A Vision for UUV Development." UnderwWater Magazine. July/August 2001.

105   Zhang, A-Ping, Tao, Xiao-Ming, and Tam, Hwa-Yaw. "Effects of Microstructures of Smart Fiber Composites on Embedded Fiber Bragg Grating Sensors." Journal of Reinforced Plastics and Composites. Vol. 22. (2003): No. 14.

106   Li, Xiaochun. "Embedded fiber Bragg grating sensors in polymer structures fabricated by layerd manufacturing." Journal of Manufacturing Procsses. 2003.

107   General Dynamics Electric Boat Division. Large Object Salvage Study. Vol 1. 1965.

108   Nixon, J.H. Underwater Repair Technology. Woodhead Publishing. 2000.

109   Drewry Shipping Consultants LTD. <u>Deep-Sea Towage, Salvage and Heavy Lift Markets</u>. 1992.

110   Transportation Research Board. "Marine Salvage Capabilities, Responding to Terrorist Attacks in U.S. Ports – Actions to Improve Readiness." National Academy of Sciences. 2004.

111   Chiu, W.K., Rees, D., and Chalkley, P. "Designing for damage-tolerant compostie repairs." Australia: Aeronautical Research Laboratory. 1994.

112   Engels, H., and Becker, W. "Closed-form analysis of external patch repairs of laminates." Germany: Universitat Siegen. 2002.

113   Kradinov, V., Hanauska, J., Barut, A., Madenci, E., and Ambur, D.R. "Bolted patch repair of composite panels with a cutout." The University of Arizona. 2002.

114   Hu, F.Z., and Soutis, C. "Strength prediction of patch-repaired CFRP laminates loaded in compression." London: Imperial College of Science, Technology & Medicine. 2000.

115   Brighenti, Roberto. "Patch repair design optimisation for fracture and fatigue improvements of cracked plates." Italy: Univerty of Parma. 2006.

116   Moksnes, J. "Resins in construction and repair of North Sea oil structures." <u>The International Journal of Cement Composites</u>. Vol 3. (1981): No. 3.

APPENDIX: REPAIR DECISION TREE

Damage suspected

NDE

Excessive damage

Scrap

Inadequate / failure

Complex

Repair type

Simple

Moderate

Check repair scheme with manufacturer

Temp. repair

Permanent repair

Repair according to approved procedure

Approve permanent repair

Return to repair facility for permanent repair

Quality check / NDE

Satisfactory repair

Return to service